MECHANICAL AND FRACTURE BEHAVIOUR OF WATER SUBMERGED GRAPHENE NANOSHEET

A DISSERTATION

Submitted in partial fulfillment of the

Requirements for the award of the degree

of

MASTER OF TECHNOLOGY

in

MECHANICAL ENGINEERING

(With Specialization in Machine Design Engineering)

by

SAURABH S SHARMA
(17539012)

DEPARTMENT OF MECHANICAL AND INDUSTRIAL ENGINEERING
INDIAN INSTITUTE OF TECHNOLOGY ROORKEE
ROORKEE-247667 (INDIA)

MAY, 2019

INDIAN INSTITUTE OF TECHNOLOGY ROORKEE, ROORKEE

CANDIDATE'S DECLARATION

I hereby declare that the work carried out in this report entitled **"MECHANICAL AND FRACTURE BEHAVIOUR OF WATER SUBMERGED GRAPHENE NANOSHEET",** is presented on behalf of partial fulfillment of the requirement for the Dissertation of "**Master of Technology**" in Mechanical Engineering with specialization in **Machine Design Engineering** submitted to the Department of Mechanical and Industrial Engineering, Indian Institute of Technology Roorkee under the supervision of **Dr. Avinash Parashar,** Assistant professor and **Dr. R. S. Mulik,** Associate Professor, Department of Mechanical and Industrial Engineering, Indian Institute of Technology Roorkee.

Date:
Place: Roorkee

SAURABH S SHARMA
Enrollment No: 17539012
M. Tech (Machine Design)
MIED, IIT Roorkee

CERTIFICATE

This is to certify that the above statement made by the candidate is correct to the best of my knowledge and belief.

(Dr. Avinash Parashar)
Assistant Professor,
MIED, IIT Roorkee.

(Prof. R. S. Mulik)
Associate Professor,
MIED, IIT Roorkee.

ABSTRACT

In this exciting age, new materials with distinctive properties emerge and continue to pique the interest of the scientific community. Stiffness and strength are the important factors in determining stability and lifetime of any technological device, but defects which are inevitable at the time of production can alter the structural properties of any engineering material. Owing to exceptional properties and diversified field of applications, graphene has attracted tremendous attention from the researchers. Developing graphene with specific structural properties depends upon controlling the concentration and distribution of geometrical defects, either by removing or deliberately introducing them in the atomic structure. Due to the spatial scale involved in such 2D nanomaterials, experimental characterization is still a challenge for researchers. Due to these challenges, numerical techniques are emerging as a viable alternative for predicting the properties of graphene. Hence, classical mechanics based molecular dynamics (MD) simulations has been considered in this research work to study the effect of defects on the mechanical properties of graphene. Success and accuracy of any molecular dynamics based simulation entirely depends on the interatomic potential employed for estimating the interatomic forces between atoms. In this work, a systematic study has been performed with different types of interatomic potentials to simulate graphene and water in the environment of molecular dynamics. Due to ever increasing demand of clean potable water, nanomaterial based membranes are emerging as potential candidates to replace the conventional polymeric membrane for enhance efficiency of desalination system. In this thesis, molecular dynamics based simulations has been performed to study the defect formation dynamics in water submerged graphene. The work is further extended to study the structural stability and fracture toughness of water submerged graphene.

ACKNOWLEDGEMENTS

I wish to express a deep sense of gratitude and sincere most thanks to my wonderful supervisors Dr. Avinash Parashar, Assistant Professor, Department of Mechanical and Industrial Engineering and Dr. R.S. Mulik, Associate Professor, Department of Mechanical and Industrial Engineering, Indian Institute of Technology Roorkee, Roorkee for their invaluable inspiration, wholehearted co-operation, motivation and important assistance throughout the duration. I consider myself fortunate to have had the opportunity to work under their able guidance and enrich myself from their depths of knowledge.

I take this opportunity to put on records my respects to Professor BK Gandhi, HOD Department of Mechanical and Industrial Engineering Indian Institute of Technology Roorkee, for providing various facilities during course of present investigation.

I would like to especially thank my colleagues Mr. Bharat Bhushan Sharma, Mr. Akarsh Verma, Mr. Ankur Chaurasia, Ms Divya Singh and my dear friend Mr Prashant Sharma for their valuable cooperation, suggestions, help and guidance in completing all tests and dissertation. I extend my thanks to all my friends who have helped directly or indirectly for the supporting me. I remain eternally indebted to my parents, Dr SD Sharma and Dr Urmil Sharma for their uplifting inspiration, guidance and never-ending enthusiasm. My wife, Kanchan and son, Advitya for their energy, support and unlimited understanding.

Finally and most humbly, I would like to express my deepest gratitude to the Almighty lord for his blessings.

Hare Krishna.

Saurabh S Sharma
Enrollment No: 17539012
M. Tech (Machine Design)
MIED, IIT Roorkee

TABLE OF CONTENT

LIST OF FIGURES

Figure **Page**

LIST OF TABLES

Table **Page**

LIST OF PUBLICATIONS

1. **Saurabh S Sharma,** Bharat Bhushan Sharma, Avinash Parashar (2019) "Defect formation dynamics in dry and water submerged graphene nanosheets", *Mater. Res. Express*, 6 075063.
2. **Saurabh S Sharma,** Bharat Bhushan Sharma, Avinash Parashar (2019) "Mechanical and fracture behaviour of water submerged graphene", Journal of Applied Physics, JAP19-AR-00311R1 (ACCEPTED)
3. **Saurabh S Sharma,** Avinash Parashar (2019) "Fracture behaviour of graphene nanosheet submerged in water", ICANM (2019), 7th international Conference and Exhibition on Advanced and Nanomaterials, Montreal, Canada. (ACCEPTED)

Chapter 1

Introduction

Due to exceptional properties and diversified field of applications, two-dimensional (2D) nanomaterials have attracted prime attention of researchers. Among the 2D nanomaterials [1–18], graphene and h-BN are in the forefront of research, and have been studied extensively by many researchers. As compared to other 2D nanomaterials, graphene is emerging as a most promising material for future technological applications. Exceptional properties of graphene (given in table 1.1) such as mechanical strength [19,20], thermal conductivity [21,22], electrical conductivity [2], tribology [23], optical transparency [24], flame retardancy [25–27], and stable thermal, chemical and electrochemical properties [28,29] are attributed either to sp2 hybridisation state of carbon-carbon bond or honeycomb space frame structure as shown in Fig.1. Graphene has already been employ for developing technologies in diversified field such as hydrogen storage [30,31], nano-sensors [32], nano-actuators [33], field effect transistors (FET) [34–37], gigahertz oscillators [38], memory devices [36], sensors, drug deliverer [39], transparent conductive films [40], graphene field emission (FE) [40], clean energy devices [34], graphene-based gas and bio sensors [41–46], graphene anodes, transparent electrodes, battery [42,47], super capacitors [47], pseudo capacitors [47], electrical double layer capacitors (EDLCs) [47], solar cells [47,48], energy production and storage [47–50], lasers protection [51], desalination membrane [52], gas barrier [53], optoelectronic applications [37] and room temperature humidity sensing applications [54]. Graphene is also listed among the potential nanofillers for developing nanocomposites with improved mechanical properties, thermal and electrical conductivities [36,47,55–59].

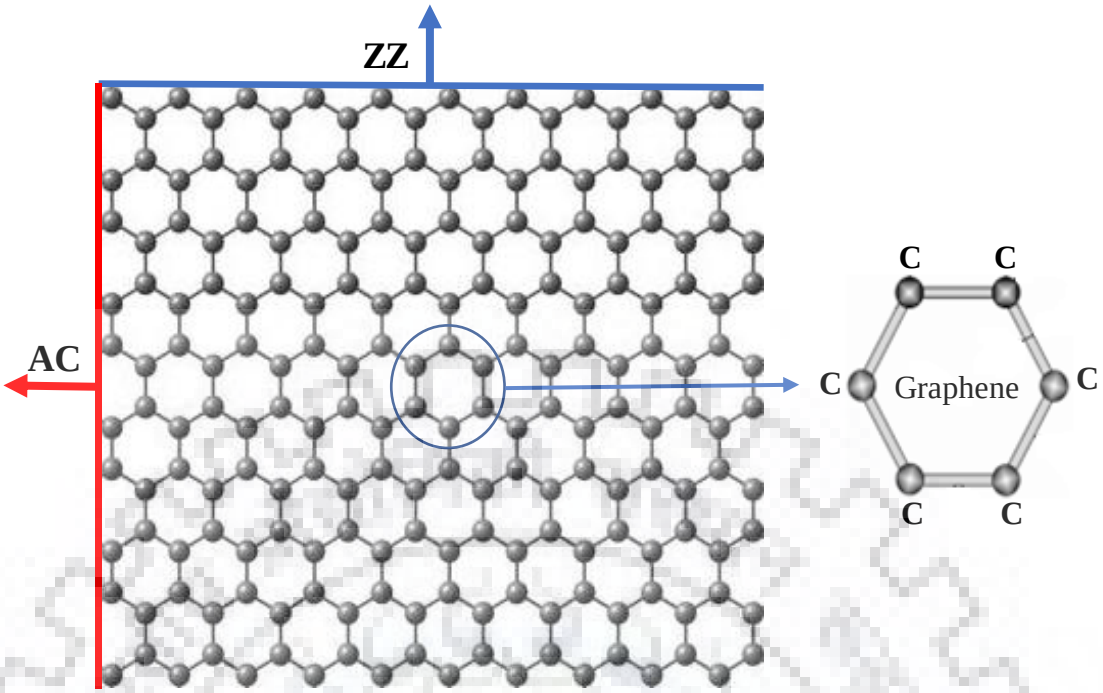

Fig.1.1 Atomic configurations of graphene nanosheet. AC and ZZ correspond to armchair and zigzag directions, respectively.[73]

Table 1.1 Properties of single crystalline graphene and h-BN nanosheets

Property	*Graphene*
Color	Black [21]
Bond length (Å)	1.42 [21]
Young's modulus (TPa)	~ 1 [60]
Failure strength (GPa)	~ 130 [60]
Shear modulus (GPa)	280 [61]
Mode I Fracture toughness $(MPa\sqrt{m})$	~ 4 [62]
Thermal conductivity $(W\,m^{-1}\,K^{-1})$	~ 5000 [63]
Thermal stability (^{o}C)	~ 500 [64]
Band gap (eV)	0 [65]
Specific surface area $(m^2 g^{-1})$	2630 [34]

In order to extend the application of these 2D nanosheets, researchers are now working on synthesising 2D nanomaterials with at-least one dimension in the range of micro meters. There is a wide range of techniques for the synthesizing of graphene and h-BN nanosheets, which allow flexibility of choices in terms of quality, size and volume of production. Some of the universal techniques used by the researchers for synthesizing graphene are chemical vapour deposition (CVD) [42,65–67], micromechanical cleavage [42,66,68], laser ablation [69], epitaxial growth of graphene on SiC [66], arc discharge [68], molecular beam epitaxy [66], and chemical exfoliation [42,65,66,70]. Generally, large size graphene and h-BN nanosheets are synthesized by the chemical vapor deposition (CVD) technique, but due to multiple nucleating sites, resulted morphology is polycrystalline instead of pristine nanosheets.

During the synthesis of these nanomaterials, either inadvertently or intentionally geometrical defects are introduced. Sometimes, researchers are intentionally introducing defects to tailor failure morphology or fracture toughness of these nanomaterials [71–79]. In larger size graphene and h-BN nanosheets, tilt GB structures are the common type of geometrical defects. Atomic configuration of GB structures in graphene and h-BN nanosheets are illustrated in Fig. 2. Building block of GB's are pair of pentagon and heptagon structures as shown in Fig.2 [80].

In larger size graphene, tilt GB structures are the common type of geometrical defects. Atomic configuration of GB structures in graphene nanosheets with pair of pentagon and heptagon structures are illustrated in Fig.1.2

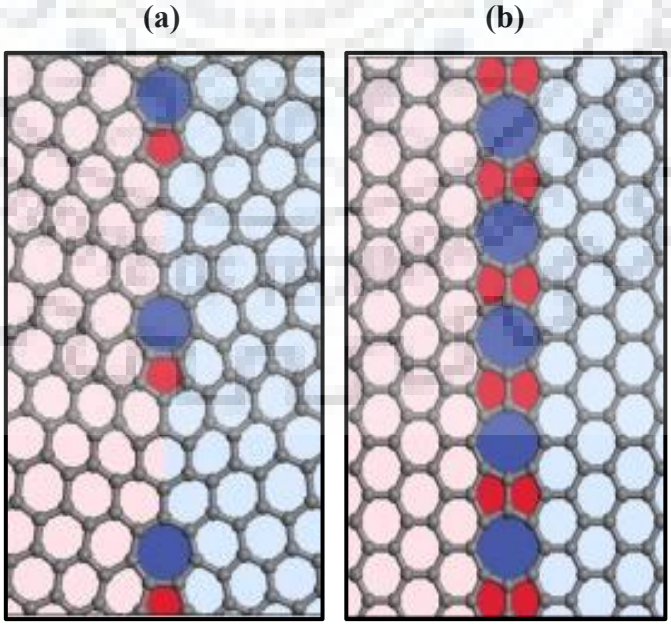

Fig.1.2 Atomic configuration of grain boundaries in (a) zigzag-oriented graphene (b) armchair-oriented graphene [79]

1.1 Definition of problem

The application of de-salination has caught fancy of world-wide research community. Need of the hour, fresh potable water, is very much likely to be fulfilled in near future by utilising RO plants. Better quality with extended shelf life can be obtained if futuristic materials like graphene are used. Extensive amount of research has already been performed with pristine as well as 2D nanomaterials (graphene nanosheets). Now, researchers are focusing on synthesizing these nanosheets with dimensions in the range of micrometres, which limits them to polycrystalline structure but increases their utility.

1.2 Objective of work

Primary focus of my dissertation was to find out behaviour of graphene in fluidic media (water) and understand its mechanical properties. Molecular dynamics-based simulations would be performed in conjunction with AIREBO and ReaxFF and TiP3P potentials to simulate graphene submerged in water model. Simulations would be performed to study the effect of defects such as cracks and vacancies on the mechanical properties, fracture toughness and failure morphology of graphene sheet.

1.3 References.

[1] Novoselov K S, Geim A K, Morozov S V., Jiang D, Zhang Y, Dubonos S V., Grigorieva I V. and Firsov A A 2004 Electric Field Effect in Atomically Thin Carbon Films *Science (80-.).* **306** 666–9

[2] Geim A K and Novoselov K S 2007 The rise of graphene *Nat. Mater.* **6** 183

[3] Dávila M E, Xian L, Cahangirov S, Rubio A and Le Lay G 2014 Germanene: A novel two-dimensional germanium allotrope akin to graphene and silicene *New J. Phys.* **16**

[4] Mojumder S, Amin A Al and Islam M M 2015 Mechanical properties of stanene under uniaxial and biaxial loading: A molecular dynamics study *J. Appl. Phys.* **118**

[5] Gusmão R, Sofer Z and Pumera M 2017 Black Phosphorus Rediscovered: From Bulk Material to Monolayers *Angew. Chemie - Int. Ed.* **56** 8052–72

[6] Radisavljevic B, Radenovic A, Brivio J, Giacometti V and Kis A 2011 Single-layer MoS2transistors *Nat. Nanotechnol.* **6** 147–50

[7] Wang Q H, Kalantar-Zadeh K, Kis A, Coleman J N and Strano M S 2012 Electronics and optoelectronics of two-dimensional transition metal dichalcogenides *Nat. Nanotechnol.* **7** 699–712

[8] Wu J, Cao P, Zhang Z, Ning F, Zheng S, He J and Zhang Z 2018 Grain-Size-Controlled Mechanical Properties of PolycryGstalline Monolayer MoS2 *Nano Lett.* **18** 1543–52

[9] Wang J, Ma F and Sun M 2017 Graphene, hexagonal boron nitride, and their heterostructures: properties and applications *RSC Adv.* **7** 16801–22

[10] Verma A, Parashar A and Packirisamy M 2017 Atomistic modeling of graphene/hexagonal boron nitride polymer nanocomposites: A review *Wiley Interdiscip. Rev. Comput. Mol. Sci.* **1346** 1–50

[11] Berger C, Song Z, Li X, Wu X, Brown N, Naud C, Mayou D, Li T, Hass J, Marchenkov A N, Conrad E H, First P N and de Heer W A 2006 Electronic Confinement and Coherence in Patterned Epitaxial Graphene *Science (80-.).* **312** 1191 LP – 1196

[12] Castro E V., Novoselov K S, Morozov S V., Peres N M R, Dos Santos J M B L, Nilsson J, Guinea F, Geim A K and Neto A H C 2007 Biased bilayer graphene: Semiconductor with a gap tunable by the electric field effect *Phys. Rev. Lett.* **99** 8–11

[13] Zhang Y, Tan Y-W, Stormer H L and Kim P 2005 Experimental observation of the quantum Hall effect and Berry's phase in graphene *Nature* **438** 201

[14] Zhang Y, Tang T T, Girit C, Hao Z, Martin M C, Zettl A, Crommie M F, Shen Y R and Wang F 2009 Direct observation of a widely tunable bandgap in bilayer graphene *Nature* **459** 820–3

[15] Golberg D, Bando Y, Huang Y, Terao T, Mitome M, Tang C and Zhi C 2010 Boron Nitride Nanotubes and Nanosheets *ACS Nano* **4** 2979–93

[16] Jin C, Lin F, Suenaga K and Iijima S 2009 Fabrication of a freestanding boron nitride single layer and Its defect assignments *Phys. Rev. Lett.* **102** 3–6

[17] Lin H and Wang X 2016 Epitaxy of Radial High-Energy-Facetted Ultrathin TiO2Nanosheets onto Nanowires for Enhanced Photoreactivities *Adv. Funct. Mater.* **26** 1580–9

[18] Zhao J, Liu H, Yu Z, Quhe R, Zhou S, Wang Y, Liu C C, Zhong H, Han N, Lu J, Yao Y and Wu K 2016 Rise of silicene: A competitive 2D material *Prog. Mater. Sci.* **83** 24–151

[19] Chang I-L and Chen J-A 2015 The molecular mechanics study on mechanical properties of graphene and graphite *Appl. Phys. A* **119** 265–74

[20] Degefe M and Parashar A 2016 Effect of non-bonded interactions on failure morphology of a defective graphene sheet *Mater. Res. Express* **3**

[21] Singh V, Joung D, Zhai L, Das S, Khondaker S I and Seal S 2011 Graphene based materials: Past, present and future *Prog. Mater. Sci.* **56** 1178–271

[22] Berman D, Erdemir A and Sumant A V. 2014 Graphene: A new emerging lubricant *Mater. Today* **17** 31–42

[23] Li Y, Wang S and Wang Q 2017 Enhancement of tribological properties of polymer composites reinforced by functionalized graphene *Compos. Part B Eng.* **120** 83–91

[24] Gwizdała W, Górny K and Gburski Z 2011 The dynamics of 4-cyano-4-n-pentylbiphenyl (5CB) mesogen molecules located between graphene layers - MD study *Spectrochim. Acta - Part A Mol. Biomol. Spectrosc.* **79** 701–4

[25] Huang G, Chen S, Tang S and Gao J 2012 A novel intumescent flame retardant-functionalized graphene: Nanocomposite synthesis, characterization, and flammability properties *Mater. Chem. Phys.* **135** 938–47

[26] Guan F L, Gui C X, Zhang H Bin, Jiang Z G, Jiang Y and Yu Z Z 2016 Enhanced thermal conductivity and satisfactory flame retardancy of epoxy/alumina composites by combination with graphene nanoplatelets and magnesium hydroxide *Compos. Part B Eng.* **98** 134–40

[27] Huang G, Gao J, Wang X, Liang H and Ge C 2012 How can graphene reduce the flammability of polymer nanocomposites? *Mater. Lett.* **66** 187–9

[28] Shahil K M F and Balandin A A 2012 Graphene-multilayer graphene nanocomposites as highly efficient thermal interface materials *Nano Lett.* **12** 861–7

[29] Parveen N, Mahato N, Ansari M O and Cho M H 2016 Enhanced electrochemical

behavior and hydrophobicity of crystalline polyaniline@graphene nanocomposite synthesized at elevated temperature *Compos. Part B Eng.* **87** 281–90

[30] Tozzini V and Pellegrini V 2013 Prospects for hydrogen storage in graphene *Phys. Chem. Chem. Phys.* **15** 80–9

[31] Verma A and Parashar A 2017 The effect of STW defects on the mechanical properties and fracture toughness of pristine and hydrogenated graphene *Phys. Chem. Chem. Phys.* **19** 16023–37

[32] Allen B L, Kichambare P D and Star A 2007 Carbon nanotube field-effect-transistor-based biosensors *Adv. Mater.* **19** 1439–51

[33] Fennimore a M, Yuzvinsky T D, Han W and Zettl a 2003 Rotational actuators based on carbon nanotubes *Nature* **424** 408–10

[34] Zhu Y, Murali S, Cai W, Li X, Suk J W, Potts J R and Ruoff R S 2010 Graphene and graphene oxide: Synthesis, properties, and applications *Adv. Mater.* **22** 3906–24

[35] Banwaskar M R and Dachawar S N 2012 Graphene Basics and Applications *Adv. Mater. Res.* **622–623** 259–62

[36] Avouris P and Dimitrakopoulos C 2012 Graphene: Synthesis and applications *Mater. Today* **15** 86–97

[37] Huang X, Yin Z, Wu S, Qi X, He Q, Zhang Q, Yan Q, Boey F and Zhang H 2011 Graphene-based materials: Synthesis, characterization, properties, and applications *Small* **7** 1876–902

[38] Cumings J and Zettl A 2000 Low-Friction Nanoscate Linear Bearing Realized from Multiwall Carbon Nanotubes *Sci. - Int. Ed. - AAAS* **289** 602–3

[39] Bianco A, Kostarelos K and Prato M 2005 Applications of carbon nanotubes in drug delivery *Curr. Opin. Chem. Biol.* **9** 674–9

[40] Rajasekaran G, Narayanan P and Parashar A 2016 Effect of Point and Line Defects on Mechanical and Thermal Properties of Graphene: A Review *Crit. Rev. Solid State Mater. Sci.* **41** 47–71

[41] Sakhaee-Pour A, Ahmadian M T and Vafai A 2008 Potential application of single-

layered graphene sheet as strain sensor *Solid State Commun.* **147** 336–40

[42] Choi W, Lahiri I, Seelaboyina R and Kang Y S 2010 Synthesis of Graphene and Its Applications: A Review *Crit. Rev. Solid State Mater. Sci.* **35** 52–71

[43] Kuila T, Bose S, Khanra P, Mishra A K, Kim N H and Lee J H 2011 Recent advances in graphene-based biosensors *Biosens. Bioelectron.* **26** 4637–48

[44] Artiles M S, Rout C S and Fisher T S 2011 Graphene-based hybrid materials and devices for biosensing *Adv. Drug Deliv. Rev.* **63** 1352–60

[45] Pumera M 2011 Graphene in biosensing *Mater. Today* **14** 308–15

[46] Ebrahimi S, Montazeri A and Rafii-Tabar H 2013 Molecular dynamics study of the interfacial mechanical properties of the graphene-collagen biological nanocomposite *Comput. Mater. Sci.* **69** 29–39

[47] Sun Y, Wu Q and Shi G 2011 Graphene based new energy materials *Energy Environ. Sci.* **4** 1113

[48] Li M, Feng Y Y, Liu E Z, Qin C Q and Feng W 2016 Azobenzene/graphene hybrid for high-density solar thermal storage by optimizing molecular structure *Sci. China Technol. Sci.* **59** 1383–90

[49] Pumera M 2011 Graphene-based nanomaterials for energy storage *Energy Environ. Sci.* **4** 668–74

[50] Brownson D A C, Kampouris D K and Banks C E 2011 An overview of graphene in energy production and storage applications *J. Power Sources* **196** 4873–85

[51] Wang J, Chen Y, Li R, Dong H, Ju Y, He J, Fan J, Wang K, Liao K S, Zhang L, Curran S A and Blau W J 2011 Graphene and Carbon Nanotube Polymer Composites for Laser Protection *J. Inorg. Organomet. Polym. Mater.* **21** 736–46

[52] Chen Q and Yang X 2015 Pyridinic nitrogen doped nanoporous graphene as desalination membrane: Molecular simulation study *J. Memb. Sci.* **496** 108–17

[53] Liu H, Bandyopadhyay P, Kshetri T, Kim N H, Ku B C, Moon B and Lee J H 2017 Layer-by-layer assembled polyelectrolyte-decorated graphene multilayer film for hydrogen gas barrier application *Compos. Part B Eng.* **114** 339–47

[54] Huang Q, Zeng D, Tian S and Xie C 2012 Synthesis of defect graphene and its application for room temperature humidity sensing *Mater. Lett.* **83** 76–9

[55] Zhan G-D, Kuntz J D, Wan J and Mukherjee A K 2002 Single-wall carbon nanotubes as attractive toughening agents in alumina-based nanocomposites *Nat. Mater.* **2** 38

[56] Kuilla T, Bhadra S, Yao D, Kim N H, Bose S and Lee J H 2010 Recent advances in graphene based polymer composites *Prog. Polym. Sci.* **35** 1350–75

[57] Das T K and Prusty S 2013 Graphene-Based Polymer Composites and Their Applications *Polym. Plast. Technol. Eng.* **52** 319–31

[58] Verdejo R, Bernal M M, Romasanta L J and Lopez-Manchado M A 2011 Graphene filled polymer nanocomposites *J. Mater. Chem.* **21** 3301–10

[59] Parashar A and Mertiny P 2013 Effect of van der waals forces on the buckling strength of graphene *J. Comput. Theor. Nanosci.* **10** 2626–30

[60] Wang M C, Yan C, Ma L, Hu N and Chen M W 2012 Effect of defects on fracture strength of graphene sheets *Comput. Mater. Sci.* **54** 236–9

[61] Liu X, Metcalf T H, Robinson J T, Houston B H and Scarpa F 2012 Shear Modulus of Monolayer Graphene Prepared by Chemical Vapor Deposition *Nano Lett.* **12** 1013–7

[62] Zhang T, Li X and Gao H 2015 Fracture of graphene: a review *Int. J. Fract.* **196** 1–31

[63] Balandin A A, Ghosh S, Bao W, Calizo I, Teweldebrhan D, Miao F and Lau C N 2008 Superior Thermal Conductivity of Single-Layer Graphene *Nano Lett.* **8** 902–7

[64] Nan H Y, Ni Z H, Wang J, Zafar Z, Shi Z X and Wang Y Y 2013 The thermal stability of graphene in air investigated by Raman spectroscopy *J. Raman Spectrosc.* **44** 1018–21

[65] Novoselov K S, Fal'Ko V I, Colombo L, Gellert P R, Schwab M G and Kim K 2012 A roadmap for graphene *Nature* **490** 192–200

[66] J. H. Warner, F. Schaffel, A. Bachmatiuk and M H R 2012 *Graphene: Fundamentals and Emergent Applications* (New York: Elsevier)

[67] Rao C N R, Sood A K, Subrahmanyam K S and Govindaraj A 2009 Graphene: The new

two-dimensional nanomaterial *Angew. Chemie - Int. Ed.* **48** 7752–77

[68] Edwards R S and Coleman K S 2013 Graphene synthesis: relationship to applications *Nanoscale* **5** 38–51

[69] Kazemizadeh F and Malekfar R 2018 One step synthesis of porous graphene by laser ablation: A new and facile approach *Phys. B Condens. Matter* **530** 236–41

[70] Papageorgiou D G, Kinloch I A and Young R J 2017 Mechanical properties of graphene and graphene-based nanocomposites *Prog. Mater. Sci.* **90** 75–127

[71] Kumar R and Parashar A 2017 Dislocation assisted crack healing in h-BN nanosheets *Phys. Chem. Chem. Phys.* **19** 21739–47

[72] Rajasekaran G and Parashar A 2017 Enhancement of fracture toughness of graphene via crack bridging with stone-thrower-wales defects *Diam. Relat. Mater.* **74** 90–9

[73] Kumar R and Parashar A 2017 Fracture toughness enhancement of h-BN monolayers via hydrogen passivation of a crack edge *Nanotechnology* **28**

[74] Kumar R, Parashar A and Mertiny P 2018 Displacement thresholds and knock-on cross sections for hydrogenated h-BN monolayers *Comput. Mater. Sci.* **142** 82–8

[75] Verma A and Parashar A 2018 Molecular dynamics based simulations to study failure morphology of hydroxyl and epoxide functionalised graphene *Comput. Mater. Sci.* **143** 15–26

[76] Rajasekaran G and Parashar A 2016 Molecular dynamics study on the mechanical response and failure behaviour of graphene: performance enhancement via 5–7–7–5 defects *RSC Adv.* **6** 26361–73

[77] Rajasekaran G and Parashar A 2016 Anisotropic compressive response of Stone-Thrower-Wales defects in graphene: A molecular dynamics study *Mater. Res. Express* **3**

[78] Verma A and Parashar A 2018 Molecular dynamics based simulations to study the fracture strength of monolayer graphene oxide *Nanotechnology* **29**

[79] Kumar R and Parashar A 2018 Effect of geometrical defects and functionalization on the interfacial strength of h-BN/polyethylene based nanocomposite *Polym. (United*

Kingdom) **146** 82–90

[80] Yazyev O V. and Louie S G 2010 Topological defects in graphene: Dislocations and grain boundaries *Phys. Rev. B - Condens. Matter Mater. Phys.* **81** 1–7

Chapter 2

Characterizing techniques

Characterization techniques for nanomaterials can be classified broadly under two sections, experimental and computational based methods as illustrated with the help of schematic in Fig 2.1. Each of these characterization techniques has certain advantages and challenges associated with them, which is discussed in the section followed.

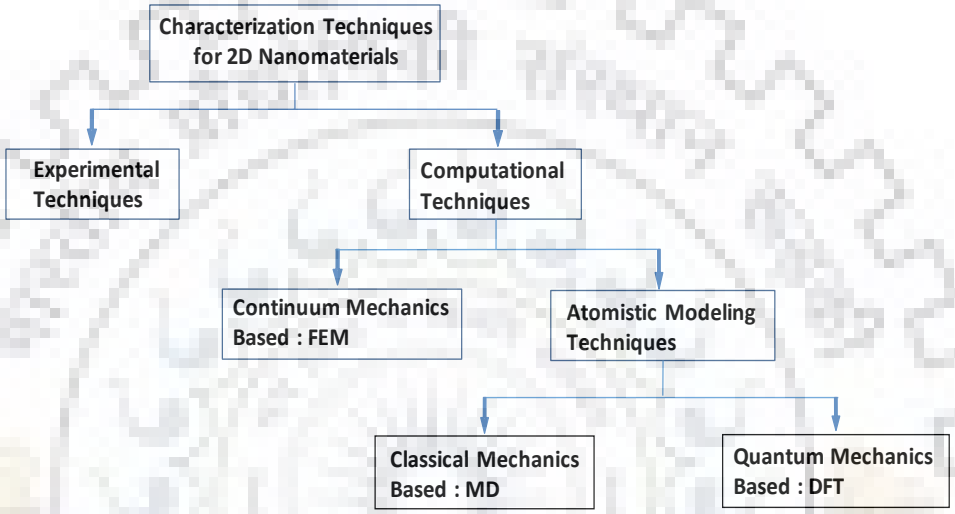

Fig 2.1 A schematic of characterizing techniques for nanomaterials

2.1 Experimental approach

Amelinckx et al. [1,2] was among the first few researchers, employed transmission electron microscopy (TEM) to observe dislocation formation in graphite. Later in the year 2004, Hashimoto and his research group also employed TEM based techniques to study the formation and distribution of dislocations in graphene [3]. First experimental studies on polycrystalline graphene and h-BN was published in the year 2011 [4–8]. TEM (high resolution and dark field) is emerging as most powerful and widely used technique to investigate the polycrystalline morphology in graphene and h-BN nanosheets [7,9–13]. Apart from TEM, scanning electron microscopy (SEM) [8], scanning tunneling microscopy (STM) [14–17], scanning tunneling spectroscopy (STS) [16,17], Raman spectroscopy [16], X-ray diffraction (XRD) [13,17], atomic force microscope (AFM) [8,16,17,18], X-ray photoelectron spectroscopy [18,20] and near edge X-ray absorption fine structure spectroscopy [21] are other standard experimental techniques that are widely used to characterize polycrystalline 2D nanomaterial's. Despite the

fact that experimental techniques are costly and time consuming, but still they are among the most accurate and realistic in nature. In addition to cost and time, experimental techniques have limitations in capturing the physics at the localized atomistic level, whereas in these nanomaterial's deformation mechanics is governed by the bond dynamics. Due to these limitations associated with experimental techniques, researchers are motivated to explore computational techniques as viable alternative to experiments.

2.2 Structural mechanics-based approach

The computational techniques can be further classified as atomistic and continuum mechanics-based techniques. The atomistic techniques include classical mechanics based molecular dynamics (MD) and quantum mechanics based density functional theory (DFT), whereas the continuum mechanics based approach mainly consists of classical continuum mechanics based finite element method (FEM) [22–25]. Already, so many research articles have been published on modelling of graphene and h-BN nanosheets with the help of structural mechanics-based approaches. In 2003, Li and Chou [23] proposed a structural mechanics based approach to simulate the deformation in single and multiple carbon nanotubes (CNT). This work is considered as a pioneer research in the field of continuum based atomistic modelling of nanomaterials.

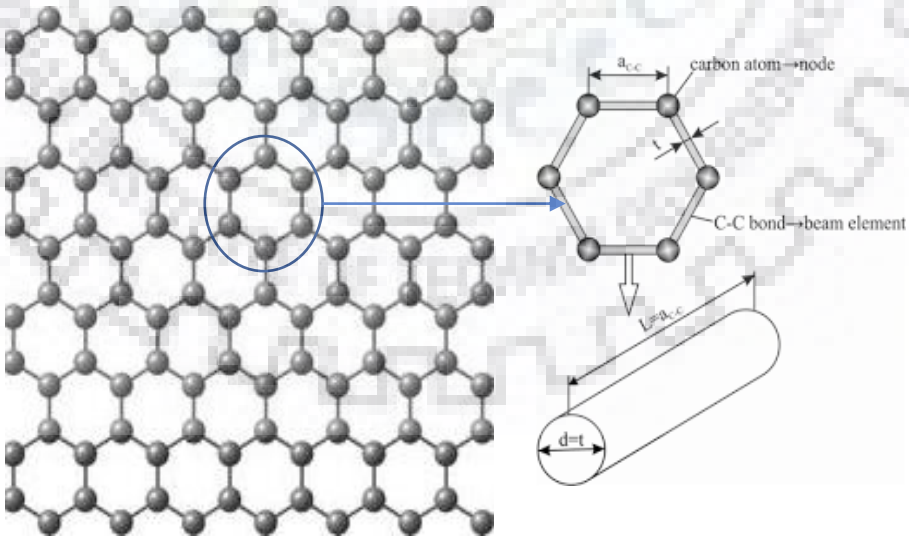

Fig 2.2 Molecular and equivalent finite element models of the graphene nanosheets[30]

Fundamental of this model was based on the notion that the atomic configuration of CNT and graphene can be simulated as space frame structure. In structural mechanics-based approach, the primary bonds between two nearest neighbouring atoms act like load bearing beam elements, whereas individual atom acts as the joint of the related load bearing beam elements or nodes. The properties of these beam elements are extracted from establishing a simple linkage between the structural and molecular mechanics. In their structural mechanics-based approach, the motion of atomic nuclei is regulated with the help of force field and this force field is generally expressed as the steric potential energy, which depends on the relative position of atomic nuclei. These structural mechanics based modelling techniques have also been extended by researchers for the modelling of 2D nanomaterials such as graphene and h-BN nanosheets [26–32]. In addition to these FEM based models of nanofillers, researchers have also used structural mechanics-based approach in conjunction with FEM to simulate mechanical and fracture properties of nanocomposites. In order to model the nanocomposite in the framework of FEM, researchers have mostly developed representative volume element (RVE), consisting of single fiber, matrix and a region in between as interface [30,31]. In FEM framework, beam, truss and continuum 3D elements are commonly used to mesh bonds, interface and matrix, respectively as shown in Fig 2.3

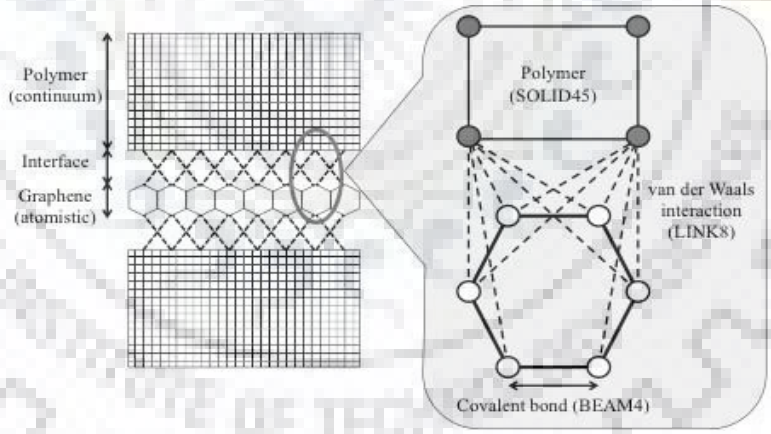

Fig 2.3 Schematic diagram of a multiscale model to simulate a nanocomposite [30]

Continuum mechanics-based approach has extensively been used by the researchers to characterise mechanical properties, fracture toughness and thermal conductivity of nanofillers and corresponding nanocomposites. Despite all these research work, continuum-based approach is limited to predicting the global or average properties, and has limitations in capturing the localised bond dynamics in these nanomaterials. On the other hand, in nanomaterials the properties are mainly governed by the physics involved at the local bond

level. Due to significant improvement in the computational facilities, researchers are substituting continuum-based approach with other atomistic level techniques such as quantum-based density functional theory and classical mechanics based molecular dynamics, which are able to capture the localised properties as well.

2.3 Density Functional Theory (DFT)

Quantum mechanics based density functional theory (DFT) is considered as most accurate among the other computational techniques. The fundamental equation (Schrödinger equation) for the electronic wave functions in presence of potential field generated by stationary atoms is solved in quantum mechanics framework. In quantum mechanics based approaches, atomic nuclei is considered as static, while the electrons are considered as moveable in the electrostatic field generated by the nuclei. In DFT based calculations, electron density is the key parameter that plays an imperative role in determining the total energy of atomic system. This total energy E[ρ], as a functional of the electron energy density 'ρ' is expressed in Eq. (1):

$$E[\rho] = T[\rho] + E_H[\rho] + E_{xc}[\rho] + E_{ext}[\rho] + E_{zz} \quad (1)$$

Where $T[\rho], E_H[\rho], E_{xc}[\rho], E_{ext}[\rho]\ and\ E_{zz}$ are the energy contributions from kinetic energy of non-interacting electrons, Hartree energy, exchange–correlation energy, external potential energy (here due to the potential of nuclei) and ion energy (due to interactions among nuclei), respectively. Solving Schrödinger equation without approximations is a tedious and highly computationally intensive task, hence, Kohn Sham (KS) [33,34] has proposed a simplified form of the equation for performing DFT calculations, which provides relatively good approximation to the energy calculations. In KS method, a problem of many interacting particles is curtailed into an equivalent fictitious problem of non-interacting particles. KS equations for this new system model are given by Eq. (2) and (3):

$$\left[-\frac{1}{2}\nabla^2 + V_{eff}(r)\right]\varphi_i(r) = \epsilon_i\varphi_i \quad (2)$$

Where

$$V_{eff} = \frac{\delta(E_H[\rho]+E_{xc}[\rho]+E_{ext}[\rho])}{\delta\rho} = V_H[\rho] + V_{xc}[\rho] + V_{ext}[\rho] \quad (3)$$

and is known as KS or effective potential, φ_i are the KS one electrons orbitals whereas electron density $\rho(r)$ is given by Eq. (4):

$$\rho(r) = \sum_{i=1}^{N}|\varphi_i|^2 \quad (4)$$

In order to solve KS equations, an initial guess of electron density "ρ" is required, which is further converged to the final electron density values after certain number of iterations. In a solid state system, the pseudopotentials (PP) [34] are used for defining interactions between core and valence electrons. After solving the KS equations, the electron density is obtained and is used to calculate the total ground state energy of the whole system. This procedure of solving KS equations is repeated until a self-consistent solution is achieved. This optimized total ground state energy is used to estimate the other structural properties of the material.

Strain energy (U) obtained from DFT based simulations (as illustrated by Eq. 5) are further processed to estimate the mechanical properties of the system.

$$U = U_{\varepsilon} - U_{\varepsilon=0} \tag{5}$$

Where, U_{ε} and $U_{\varepsilon=0}$ are the strain/ potential energy of the strained and unstrained atomistic system respectively and this strain energy is again processed to predict Young's modulus (Y in Nm^{-2}) and 2D Young's modulus (Y_S in Nm^{-1}) as demonstrated in Eq. (6) and (7) respectively:

$$Y = (\partial^2 U/\partial \varepsilon^2)/V \tag{6}$$

$$Y_S = (\partial^2 U/\partial \varepsilon^2)/S \tag{7}$$

Here, V and S are volume and surface area respectively.

Although, the DFT based technique are widely used technique for the atomistic simulations performed with limited number of atoms. Due to computationally intensive calculations, DFT based simulations are limited to estimate binding energies, defect formation energies and properties that can be estimated with the help of limited number of atoms in the range of hundreds and thousands. These days' researchers are using DFT simulations in multiscale modeling techniques, where limited part of the atoms are dealt with DFT, whereas the remaining with less computational intensive technique such as molecular dynamics [35].

2.4 Molecular Dynamics

Molecular dynamics (MD) based technique is another emerging alternative to perform atomistic simulations. MD is already considered a powerful tool for simulation in the field of biological and chemical science. In the last few years, application of MD based simulations has been extended in the field of material science to predict properties of conventional as well as non-conventional materials. MD is a widely used semi empirical computer based atomistic

simulation technique of atoms/molecules in the context of N-body systems. In MD based simulations atoms are treated as classical particles, and interaction between them is estimated with the help of empirically derived interatomic potentials. Relationship derived from the Newton's second law of motion is used for updating the position, velocity and acceleration of each atom in the system with respect to integration time steps. The fundamental equation (Eq.8) solved in MD based simulation is given as:

$$m_\alpha a_\alpha = F_\alpha = -(\partial E / \partial r_\alpha) \quad (8)$$

where α = 1,2,……, N

Here, N is total number of atoms; m_α, r_α and F_α are mass, position and time dependent force acting on it due to external agents, respectively. The potential energy 'E' consists of an internal part (E^{int}) that accounts for the interaction between the atoms and an external part (E^{ext}) that accounts for external fields and constraints. Potential energy (E) and force F_α are the function of position and velocity vectors of the atoms. Statistical mechanics-based approaches are commonly used over the time averages to derive macroscopic properties such as pressure, temperature, stresses etc.

In MD based simulations, position and velocity vectors are updated after each integration time step, usually by using any of the numerical integration algorithms [36–37]. Interatomic potentials/force fields (FF) form the most integral and critical part of any MD based simulation. Generalized expression for estimating the total atomic energy of the system containing α atoms is provided in Eq. (9)

$$U_{total} = \frac{1}{2}\sum_{\alpha=\beta=1}^{N}\sum_{\beta=1}^{N}\emptyset(r_{\alpha\beta}) \quad (9)$$

where, $r_{\alpha\beta}$ is the distance between particles α and β, $\emptyset(r_{\alpha\beta})$ is the potential energy between particles α and β. Interatomic potentials are empirically developed and validated either from experiments or higher fidelity numerical simulations such as DFT. They are subdivided based on positions of number of atoms taken into consideration; pair potentials (two atoms), three- and four- body potentials (three and four atoms) and cluster potentials (n atoms). In order to keep the review concise and comprehensive, brief details of commonly used interatomic potentials for 2D nanomaterial's such as graphene and h-BN is included in the dissertation. For the modelling of carbon based nanofillers, AMBER [38], chemistry at Harvard macromolecular mechanics (CHARMM) [39], L-J [40], reactive bond order (REBO) [41], adaptive interatomic

reactive bond order (AIREBO) [42], reactive force field (reaxFF) [43–45] and Tersoff type interatomic potentials [46–50] are commonly employed by the researchers.

In addition to these interatomic potentials, one more interatomic potential that is more accurate, and have the capability of capturing the bond breaking and formation is proposed by Andri Duin, is referred as reactive force field (ReaxFF). ReaxFF is a universal type force field that can be used to simulate mechanical and thermal behavior of graphene, h-BN as well as polymers with separate set of parameters [43–45,50]. Similar to other empirical non-reactive potentials, the total energy of the system is derived from various partial energy contributions (bonded as well as non-bonded) as expressed in Eq. (10).

$$E_{system} = E_{bond} + E_{over} + E_{under} + E_{lp} + E_{val} + E_{pen} + E_{tors} + E_{conj} + E_{vdWaals} + E_{Columb} \tag{10}$$

ReaxFF type potentials are reported to be more suitable for simulating bond-breaking and bond-forming mechanisms. Fundamental difference between ReaxFF and most of the other empirical interatomic potentials is that ReaxFF does not employ any fixed connectivity for the bonded interaction. In ReaxFF type potentials the bond order is directly calculated from the instantaneous interatomic distance r_{ij}, which keeps on updating during the simulation. This bond order is responsible for creation and dissociation of bonds during the simulation.

The concept of stress in a material or a body is well known at the continuum level and usually referred as Cauchy stress tensor. However, at atomistic level the principles of continuum are not applicable, and hence an alternative stress referred as virial stress is estimated at atomistic level. The virial stress is the most commonly used definition of stress in discrete particle systems. Virial stress is the summation of two components; first component depends upon the mass and velocity of the atoms (kinetic energy term), whereas the second component depends upon the interatomic forces and atomic positions. The mathematical expression for virial stress as the summation of two components is given by Eq. (11).

$$\sigma_{ij}^{\alpha} = \frac{1}{\varphi^{\alpha}}\left(\frac{1}{2}m^{\alpha}v_i^{\alpha}v_j^{\alpha} + \sum_{\beta=1,n} r_{\alpha\beta}^{j} f_{\alpha\beta}^{i}\right) \tag{11}$$

Where *i* and *j* denote indices in Cartesian coordinate system; α and β are the atomic indices; m^{α} and v^{α} are mass and velocity of atom α; $r_{\alpha\beta}$ is the distance between atoms α and β; and φ^{α} is the atomic volume of atom α.

In addition to predicting the mechanical behavior of an atomistic system, the MD based simulations are also used for predicting the thermal behavior of the atomistic system. Thermal conductivity (*k*) of a simulated atomistic configuration can be estimated by using the mathematical expressions given below:

$$k = \frac{J}{2A\left(\frac{\partial T}{\partial x}\right)} \tag{12}$$

$$J = \frac{\sum 0.5 N_{transfer}(m_h v_h^2 - m_c v_c^2)}{t_{transfer}} \tag{13}$$

Here, in Eq. (12) and (13), $\frac{\partial T}{\partial x}$ refers to the temperature gradient along the direction of heat flux (*J*), *A* is the cross-sectional area, *h* and *c* refer to the hot and cold atoms, $N_{transfer}$ and $t_{trasfer}$ are summation time and number of exchanges respectively.

After reviewing all the computational based techniques employed by researchers for the modelling of 2D nanomaterial's, it can be concluded that each of these techniques have some limitations and challenges associated with them. As compared to FEM based techniques, atomistic simulations are more suitable for the modelling of nanomaterials. Capability of capturing bond dynamics at the localized phase, with least computational efforts as compared to DFT, makes MD based simulations as the potential candidate for performing numerical simulations with 2D nanomaterials.

2.5 References.

[1] Amelinckx and Delavignette 1960 Dislocation loops due to quenched in point defects in graphite *Phys. Rev. Lett.* **5** 50

[2] Delavignette P and Amelinckx S 1962 Dislocation patterns in graphite *J. Nucl. Mater.* **5** 17–66

[3] Hashimoto A, Suenaga K, Gloter A and Urita K 2004 Direct evidence for atomic defects in graphene layers **430** 17–20

[4] Huang P Y, Ruiz-Vargas C S, Van Der Zande A M, Whitney W S, Levendorf M P, Kevek J W, Garg S, Alden J S, Hustedt C J, Zhu Y, Park J, McEuen P L and Muller D A 2011 Grains and grain boundaries in single-layer graphene atomic patchwork quilts *Nature* **469** 389–92

[5] Kim K, Lee Z, Regan W, Kisielowski C, Crommie M F and Zettl A 2011 Grain boundary mapping in polycrystalline graphene *ACS Nano* **5** 2142–6

[6] An J, Voelkl E, Suk J W, Li X, Magnuson C W, Fu L, Tiemeijer P, Bischoff M, Freitag B, Popova E and Ruoff R S 2011 Domain (Grain) boundaries and evidence of "twinlike" structures in chemically vapor deposited grown graphene *ACS Nano* **5** 2433–9

[7] Gibb A L, Alem N, Chen J, Erickson K J, Ciston J, Gautam A, Linck M and Zettl A 2013 Atomic Resolution Imaging of Grain Boundary Defects in Monolayer *J. Am. Chem. Soc.* **135** 6758–61

[8] Wu Q, Lee J, Park S, Woo H J, Lee S and Song Y J 2018 Defect-selective dry etching for quick and easy probing of hexagonal boron nitride domains *Nanotechnology* **29** 125704

[9] Ophus C, Shekhawat A, Rasool H and Zettl A 2015 Large-scale experimental and theoretical study of graphene grain boundary structures *Phys. Rev. B - Condens. Matter Mater. Phys.* **92** 205402

[10] Robertson A W and Warner J H 2013 Atomic resolution imaging of graphene by transmission electron microscopy *Nanoscale* **5** 4079

[11] Lee G-H, Cooper R C, An S J, Lee S, van der Zande A, Petrone N, Hammerberg A G, Lee C, Crawford B, Oliver W, Kysar J W and Hone J 2013 High-Strength Chemical-Vapor-Deposited Graphene and Grain Boundaries *Science* **340** 1073–6

[12] Rasool H I, Ophus C, Klug W S, Zettl A and Gimzewski J K 2013 Measurement of the intrinsic strength of crystalline and polycrystalline graphene *Nat. Commun.* **4** 2811

[13] Hawelek L, Kolano-Burian A, Szade J, Maziarz W, Woznica N and Burian A 2013 The atomic scale structure of nanographene platelets studied by X-ray diffraction, high-resolution transmission electron microscopy and molecular dynamics *Diam. Relat.*

Mater. **35** 40–6

[14] Albrecht T R, Mizes H A, Nogami J, Park S Il and Quate C F 1988 Observation of tilt boundaries in graphite by scanning tunneling microscopy and associated multiple tip effects *Appl. Phys. Lett.* **52** 362–4

[15] Simonis P, Goffaux C, Thiry P ., Biro L ., Lambin P and Meunier V 2002 STM study of a grain boundary in graphite *Surf. Sci.* **511** 319–22

[16] Červenka J and Flipse C F J 2009 Structural and electronic properties of grain boundaries in graphite: Planes of periodically distributed point defects *Phys. Rev. B - Condens. Matter Mater. Phys.* **79** 195429

[17] Li Q, Zou X, Liu M, Sun J, Gao Y, Qi Y, Zhou X, Yakobson B I, Zhang Y and Liu Z 2015 Grain Boundary Structures and Electronic Properties of Hexagonal Boron Nitride on Cu(111) *Nano Lett.* **15** 5804–10

[18] Yao H, Liu L, Fu W, Yang H and Shi Y 2017 Fe_2O_3 nanothorns sensitized two-dimensional TiO_2 nanosheets for highly efficient solar energy conversion *FlatChem* **3** 1–7

[19] Ruiz-Vargas C S, Zhuang H L, Huang P Y, Van Der Zande A M, Garg S, McEuen P L, Muller D A, Hennig R G and Park J 2011 Softened elastic response and unzipping in chemical vapor deposition graphene membranes *Nano Lett.* **11** 2259–63

[20] Zandiatashbar A, Lee G H, An S J, Lee S, Mathew N, Terrones M, Hayashi T, Picu C R, Hone J and Koratkar N 2014 Effect of defects on the intrinsic strength and stiffness of graphene *Nat. Commun.* **5** 3186

[21] Sun Y, Gao S, Lei F, Xiao C and Xie Y 2015 Ultrathin two-dimensional inorganic materials: New opportunities for solid state nanochemistry *Acc. Chem. Res.* **48** 3–12

[22] Parashar A and Mertiny P 2012 Study of mode i fracture of graphene sheets using atomistic based finite element modeling and virtual crack closure technique *Int. J. Fract.* **176** 119–26

[23] Li C and Chou T W 2003 A structural mechanics approach for the analysis of carbon nanotubes *Int. J. Solids Struct.* **40** 2487–99

[24] Parashar A and Mertiny P 2013 Finite element analysis to study the effect of

dimensional and geometrical parameters on the stability of graphene sheets *J. Comput. Theor. Nanosci.* **10** 292–6

[25] Parashar A and Mertiny P 2013 Effect of van der Waals interaction on the mode i fracture characteristics of graphene sheet *Solid State Commun.* **173** 56–60

[26] Tserpes K I and Papanikos P 2005 Finite element modeling of single-walled carbon nanotubes *Compos. Part B Eng.* **36** 468–77

[27] Baykasoglu C and Mugan A 2012 Dynamic analysis of single-layer graphene sheets *Comput. Mater. Sci.* **55** 228–36

[28] Scarpa F, Adhikari S and Srikantha Phani A 2009 Effective elastic mechanical properties of single layer graphene sheets *Nanotechnology* **20** 065709

[29] Scarpa F, Adhikari S and Chowdhury R 2010 The transverse elasticity of bilayer graphene *Phys. Lett. Sect. A Gen. At. Solid State Phys.* **374** 2053–7

[30] Parashar A and Mertiny P 2012 Multiscale model to investigate the effect of graphene on the fracture characteristics of graphene/polymer nanocomposites *Nanoscale Res. Lett.* **7** 595

[31] Parashar A and Mertiny P 2012 Representative volume element to estimate buckling behavior of graphene/polymer nanocomposite *Nanoscale Res. Lett.* **7** 515

[32] Xu N, Guo J G and Cui Z 2016 The influence of tilt grain boundaries on the mechanical properties of bicrystalline graphene nanoribbons *Phys. E Low-Dimensional Syst. Nanostructures* **84** 168–74

[33] And W K and SHAM L J 1965 Self-Consistent Equations Including Exchange and Correlation Effects *Phys. Rev. A* **140** 1133–8

[34] Lee J G 2012 *Computational Materials Science An Introduction* (New York, USA: CRC Press)

[35] Hirvonen P, Ervasti M M, Fan Z, Jalalvand M, Seymour M, Vaez Allaei S M, Provatas N, Harju A, Elder K R and Ala-Nissila T 2016 Multiscale modeling of polycrystalline graphene: A comparison of structure and defect energies of realistic samples from phase field crystal models *Phys. Rev. B* **94** 035414

[36] Omeltchenko A, Yu J, Kalia R K and Vashishta P 1997 Crack front propagation and

fracture in a graphite sheet: A molecular-dynamics study on parallel computers *Phys. Rev. Lett.* **78** 2148–51

[37] Eastwood R W H and J W 1981 *Computer Simulation Using Particles* (New York: McGraw-Hill)

[38] Wang J M, Wolf R M, Caldwell J W, Kollman P a and Case D a 2004 Development and testing of a general amber force field *J. Comput. Chem.* **25** 1157–74

[39] MacKerell A D, Wiórkiewicz-Kuczera J, Karplus M and MacKerell A D 1995 An All-Atom Empirical Energy Function for the Simulation of Nucleic Acids *J. Am. Chem. Soc.* **117** 11946–75

[39] Jones J E 1924 On the Determination of Molecular Fields. II. From the Equation of State of a Gas *Proc. R. Soc. London* **106** 463–77

[40] Jeong B W, Lim J K and Sinnott S B 2007 Tensile mechanical behavior of hollow and filled carbon nanotubes under tension or combined tension-torsion *Appl. Phys. Lett.* **90** 023102

[41] Stuart S J, Tutein A B and Harrison J A 2000 A reactive potential for hydrocarbons with intermolecular interactions *J. Chem. Phys.* **112** 6472–86

[42] Van Duin A C T, Dasgupta S, Lorant F and Goddard W A 2001 ReaxFF: A reactive force field for hydrocarbons *J. Phys. Chem. A* **105** 9396–409

[43] van Duin A C T, Strachan A, Stewman S, Zhang Q, Xu X and Goddard W A 2003 ReaxFF $_{SiO}$ Reactive Force Field for Silicon and Silicon Oxide Systems *J. Phys. Chem. A* **107** 3803–11

[44] Weismiller M R, Duin A C T van, Lee J and Yetter R A 2010 ReaxFF Reactive Force Field Development and Applications for Molecular Dynamics Simulations of Ammonia Borane Dehydrogenation and Combustion *J. Phys. Chem. A* **114** 5485–92

[45] Tersoff J 1988 New empirical approach for the structure and energy of covalent systems *Phys. Rev. B* **37** 6991–7000

[46] Tersoff J 1988 Empirical interatomic potential for carbon, with applications to amorphous carbon *Phys. Rev. Lett.* **61** 2879–82

[47] Tersoff J 1989 Modeling solid-state chemistry: Interatomic potentials for

multicomponent systems *Phys. Rev. B* **39** 5566–8

[48] Rajasekaran G. A P 2016 Molecular dynamics based simulations to study the effect of modified cut-off function for Tersoff potential on estimating mechanical properties of graphene *Mater. Res. expres* **3** 035011

[49] Kumar R, Rajasekaran G and Parashar A 2016 Optimised cut-off function for Tersoff-like potentials for a BN nanosheet: A molecular dynamics study *Nanotechnology* **27** 085706

[50] Kumar R, Mertiny P and Parashar A 2016 Effects of Different Hydrogenation Regimes on Mechanical Properties of h-BN: A Reactive Force Field Study *J. Phys. Chem. C* **120** 21932–8

Chapter 3

Defect formation dynamics in dry and water submerged graphene nanosheets[1]

3.1 Introduction

Much of the research in the post silicon age has been carried out to develop newer and better materials. Due to exceptional mechanical, thermal and electrical properties, graphene is emerging as a strong contender to replace conventional materials [1-6]. Researchers are exploring graphene for applications in diversified and futuristic applications [7-13]. Utilization of the sp^2-hybridized structure of carbon atoms in graphene is a novel way to look forward in space technology [14], desalination and filtration membrane systems [15,16], nano-biotechnology [17], MEMS/NEMS (nanoelectromechanical systems) [18], polymer reinforcement [19,20] and smart memory devices [21]. In addition to these applications, researchers are also developing nuclear pellets for nuclear reactors [22].

Graphene nanosheets are widely produced by mechanically exfoliating flakes from bulk graphite [23], which limits the control over size and crystal quality. Alternatively, graphene has also been synthesized on various solid surfaces by chemical vapor deposition (CVD) or surface segregation techniques. These processes induce various topological defects such as grain boundaries, dislocations, vacancies and Stone-Thrower-Wales(STW) defects which are also known as 5-7-7-5 defects. The STW defects are formed when one bond of C-C atoms in hexagonal structure is rotated by 90^0 forming 2 pentagons and 2 heptagons instead of 4 adjacent hexagons as mentioned in literature [24]. Rajasekaran et al. [24] studied the effect of point defects on mechanical and thermal properties of graphene. They predicted that graphene has a

[1] This chapter is an excerpt from the article published as Saurabh S Sharma, Bharat Bhushan Sharma, Avinash Parashar, 2019, Mater. Res. Express 6 075063

unique ability to reconstruct its lattice structure by forming non-hexagonal rings. Verma et al. [25] predicted improved fracture toughness for hydrogen functionalized graphene in presence of STW defects in close vicinity of crack tip. Meng et al. [26] predicted that utilization of dislocations in graphene structure provided stress shielding effect at the crack tip. Recently, Singla et al. [27] studied the point defect formation energies in graphene containing STW defects. They found out the vacancy formation and displacement threshold energies are significantly affected in presence of STW defects. Defects such as STW, dislocations and point defects are geometrical in nature, can be synthesized chemically or introduced intentionally by ion and /or electron bombardment [28]. Yoon et al. [29] utilised noble gas ions to generate STW defects in graphene. In order to study the structural stability, Merill et al. [30] predicted the displacement threshold energies of single walled carbon nanotubes. In addition to dry form, researchers have also started exploring the mechanical behavior of graphene submerged in water [31,32]. Wong and Vijayaraghavan [31] studied the mechanical strength of water submerged graphene in conjunction with vacancy defects. In their atomistic simulations edge effects were ignored in submerged graphene. Tanugi and Grossman [32] have also investigated the mechanical strength of water submerged graphene containing nanopores with different spatial distribution.

Amid the frenzy of worldwide research on a crucial material like graphene, there is one area that has eluded any systematic analysis, even though this information could be crucial to a host of potential applications that includes desalination, DNA sequencing, and devices for quantum communications and computation systems. But, limited research has been performed with respect to defect formation energies of graphene submerged in water. In order to investigate the defect formation dynamics, authors have performed molecular dynamics (MD) based simulations in conjunction with hybrid type of potentials. In the present dissertation, overall simulations were performed in three stages, initially, vacancy formation energies (VFE) were

estimated and later on displacement threshold energies (E_d) were estimated for graphene in dry and wet forms. Finally, the grain boundary formation energies were predicted in water submerged graphene. In order to quantify the effect of water on the properties of graphene, results were compared with the pristine and dry form of graphene.

3.2 Modelling details

A classical mechanics-based approach was employed to study the defect formation dynamics in water submerged graphene. An open source code LAMMPS (Large-scale Atomic/Molecular Massively Parallel Simulator) package was used to perform all the atomistic simulations, whereas the post procession of dump files was performed with the help of open visualization tool (OVITO). In order to capture the atomistic interactions between the carbon-carbon atoms in graphene, more complex as well as accurate reactive force-field (ReaxFF) interatomic potential was utilised. ReaxFF employs a bond-order relationship in conjunction with charge descriptions to describe both reactive and non-reactive interactions between atoms [33]. The selection of this type of interatomic potential is justified as Reaxx FF is considered most accurate and next to the accuracy of quantum mechanics-based approaches like DFT (Density Functional Theory). Mathematically, energy contributions in the ReaxFF potential are summarised by the following equation:

$$\boldsymbol{E_{system} = E_{bond} + E_{over} + E_{angle} + E_{tors} + E_{vdWaals} + E_{coulomb} + E_{specific}} \quad (1)$$

Here, E_{bond} is a continuous function of interatomic distance and describes the energy associated with forming bonds between atoms. E_{over} is an energy penalty preventing the over coordination of atoms, which is based on atomic valence rules (e.g., a stiff energy penalty is applied if a carbon atom forms more than four bonds). E_{angle} and E_{tors} are the energies associated with three-body valence angle strain and four-body torsional angle strain. $E_{vdWaals}$ and $E_{coulomb}$ are

electrostatic and dispersive contributions calculated between all atoms, regardless of connectivity and bond-order. $E_{specific}$ represents system specific terms that are not generally included, unless required to capture properties particular to the system of interest, such as lone-pair, hydrogen binding and Conjugate bond corrections. In order to capture the bond dynamics between the oxygen and hydrogen atoms in water, TIP3P potential was used in all the simulations. On the other hand, non-bonded interactions between the water molecules and graphene was captured with the help of Lennard Jones potential. In order to avoid surface affects, periodic boundary conditions were imposed in all the principal directions. All the simulations were performed at the room temperature of 300K. Snapshot of the simulation box containing dry and water submerged graphene is shown in Fig.3.1

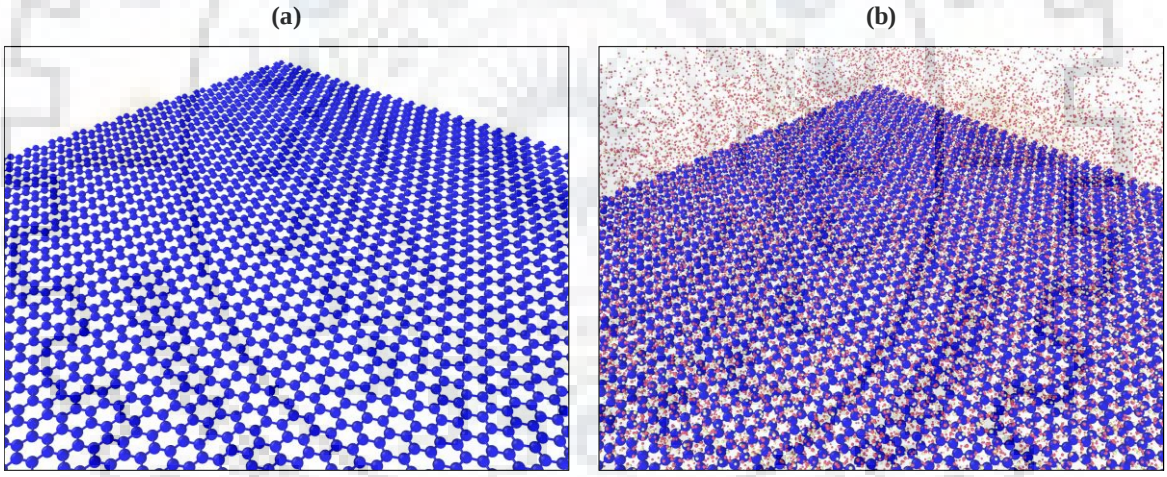

Fig.3.1 Dry and submerged graphene nanosheets, respectively.

In this dissertation, simulations were performed to predict primarily three different type of defect formation energies, vacancy formation energy (VFE), displacement threshold energy (E_d) and grain boundary formation energy (GB_E). Mathematical expression to calculate value of VFE is given in equation 2.

$$VFE = E_{Vacancy} - E_{pristine} + E_{coh} \quad (2)$$

where, $E_{Vacancy}$ and $E_{pristine}$ corresponds to potential energy of graphene containing vacancy and in pristine form without defects, respectively, and E_{coh} is cohesive energy of carbon in graphene.

Simulations to predict VFE were carried out with dry and water submerged graphene nanosheets having equal length and width ≈ 60 Å, which constitutes approximately 1344 carbon atoms. After allocating spatial coordinates to hydrogen and oxygen atoms in water molecules and carbon in graphene, minimum energy configuration was obtained with the help of conjugate gradient algorithm. After minimizing the overall atomic configuration in dry and wet form (includes water in simulation box), potential energy of graphene in pristine form and after creating vacancy was estimated, which was further used in Eq.2 to predict VFE.

Next set of simulations were performed to predict the displacement threshold energy of carbon atoms in dry and water submerged graphene nanosheets. Simulations to predict E_{d} (displacement threshold energy) were carried out under the micro-canonical (NVE) ensemble. In this simulation phase, a section of the atomistic structure consisting of central part of the defective graphene sheet with an approximate size 30×30 $Å^2$ was considered as the target atomic system, whereas the rest of sheet was used as a thermal sink to maintain the system temperature at 300 K as depicted in Fig.3.2 Temperature of the simulation box was maintained at 300K with the help of Berendsen thermostat. After relaxing the system at 300K, thermoset was released from the central portion highlighted in Fig.3.2, whereas the temperature of the region excluding central graphene nanosheet was maintained as thermal sink at 300K with the help of thermostat.

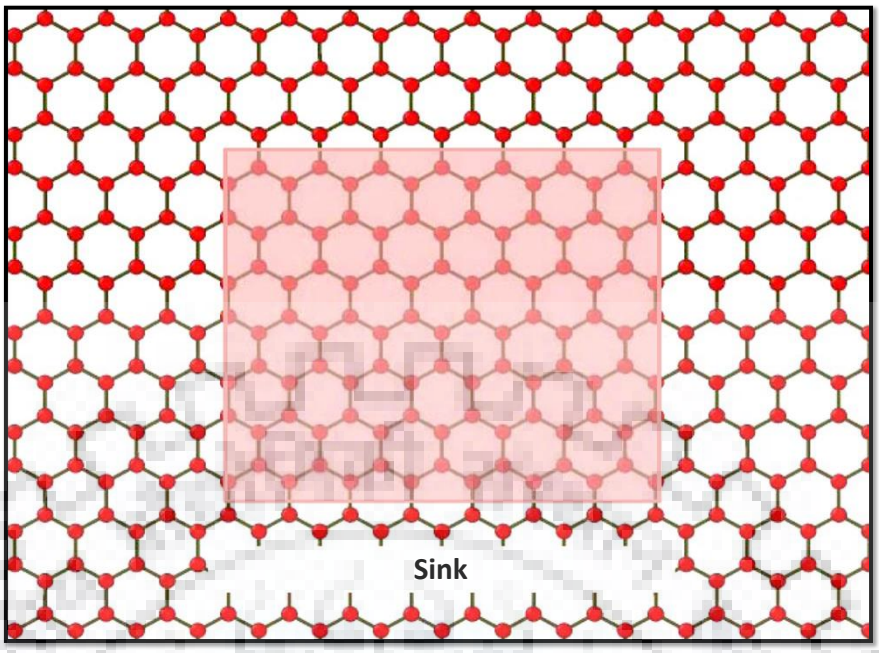

Fig.3.2 Target atomic system (shown in red coloured shaded region), while rest of the carbon monolayer sheet is kept at a constant sink temperature of 300 K.

In order to estimate the displacement threshold energy (E_d) in dry and wet form of graphene nanosheet, a primary knock on atom (PKA) was selected in the target region by imparting kinetic energy in the direction perpendicular to the graphene nanosheet. Kinetic energy was imparted in fractional increments such as the PKA was permanently dislodged from the graphene nanosheet. The velocity vector given to the PKA remained fixed in the direction perpendicular to nanosheet plane (z-direction) as shown in stages in Fig. 3.3 The minimum value of kinetic energy required to dislodge the carbon atom from lattice position in graphene was assigned to displacement threshold energy (E_d).

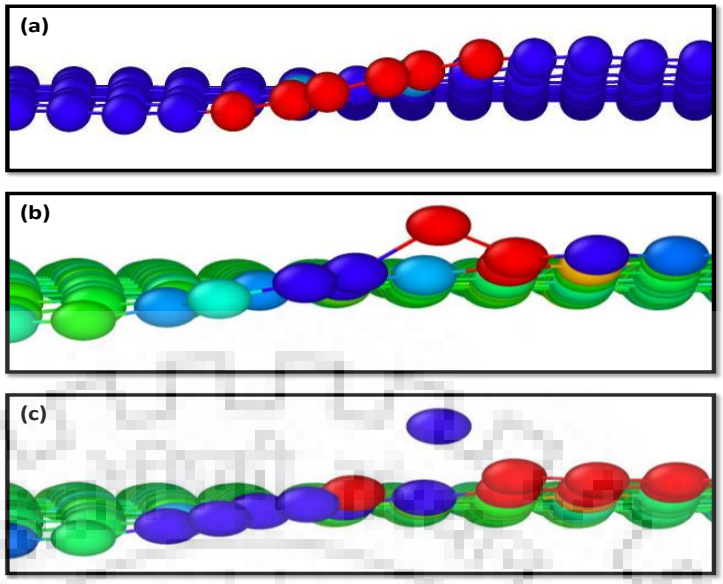

Fig. 3.3 (a) Velocity given in z+ direction to selected PKA from the central portion, (b) Target atom gaining energy and (c) Permanent damage created as the PKA atom is dislodged from its lattice position.

In the last set of simulations, symmetric tilt grain boundaries were created between crystals of graphene nanosheets. During this set of simulations, mis-orientation angle between the nanosheets were kept at 9.44^o, 13.2^o and 21.8^o. Grain boundaries consists of sets of dislocations; hence the simulations will help us in estimating the formation energies of these defects in dry as well as water submerged state [34]. Schematic of the bi-crystalline graphene containing tilt grain boundaries at different mis-orientation angles are shown in Fig.4. Grain boundary energy in dry and wet state for graphene was estimated with the help of Eq.3.

$$GB_E = E_{GB} - E_{coh} \times N \tag{3}$$

Here, GB_E and E_{GB} corresponds to grain boundary formation energy and potential energy of the bi-crystalline graphene after minimizing the energy of the system with CG algorithm. E_{coh} and N refers to cohesive energy and number of atoms in bi-crystalline graphene nanosheet.

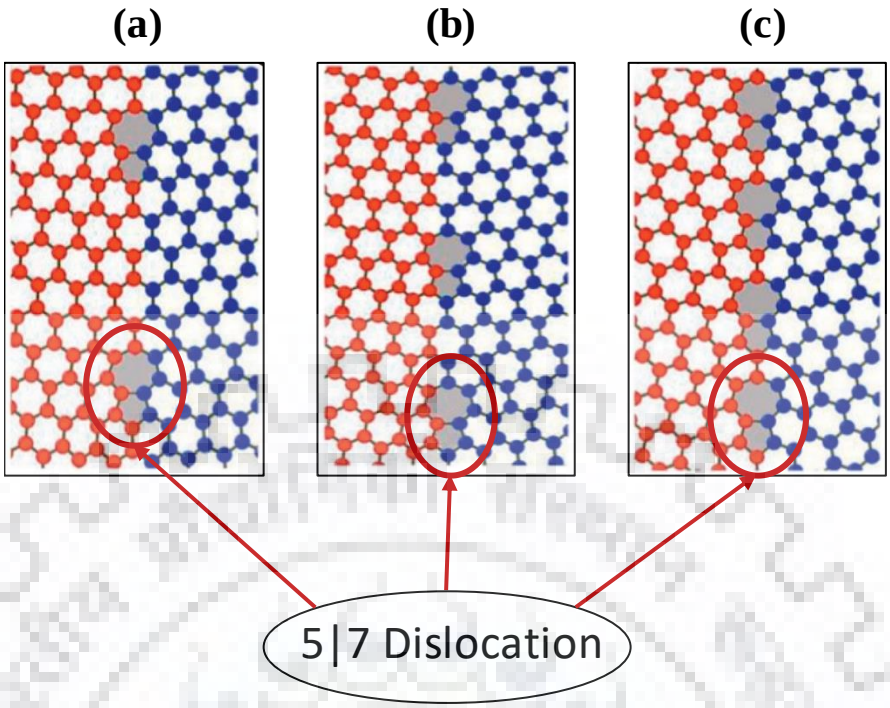

Fig. 3.4 Grain boundary configuration containing misorientation angle of (a) 9.4^0, (b) 13.2^0 and (c) 21.8^0, respectively

3.3 Results and discussions

Defect formation dynamics helps us in predicting the resistance against the defect formation and also the stability of graphene containing defects. Defect formation dynamics was studied as defects are an integral part of graphene, due to limitations associated with the manufacturing processes. Also surface topology has a strong bearing on the mechanical and thermal properties of graphene. As mentioned in the previous section, simulations were performed in three stages, stage one and two corresponds to vacancy formation energy and displacement threshold energies, whereas the third stage refers to grain boundary formation energy.

Vacancy formation energy

As mentioned in the previous section, VFE for dry (≈8.4eV) and water submerged state (≈8.0eV) of graphene was estimated with the help of Eq.2. It can be predicted from the values

of VFE in dry state that values are slightly higher than predicted by Krasheninnikov et al. [35] and Thrower & Mayer [36]. The offset in values can be attributed to the interatomic potentials used in this work was reaxFF, which is stiffer in terms of energy components as compared to the previously used potentials. It can be inferred from the VFE values in dry and wet state that graphene in dry state is more susceptible to defects as compared to wet form. It can be seen in Fig.5 that the atoms in the vicinity of vacancy are at higher energy state, but in wet state the energy of those atoms are comparatively lower. This lower value of VFE in wet state of graphene is attributed to the interaction between the graphene atoms and water molecules that helps in stabilizing the atomic configuration in the near vicinity of vacancy and reducing the overall energy of the system.

The potential energies around the vacancies are depicted in Fig.3.5 It can be observed from Fig.3.5 that the vacancy formed under water is more stable in terms of energy distribution as well as atomic configuration.

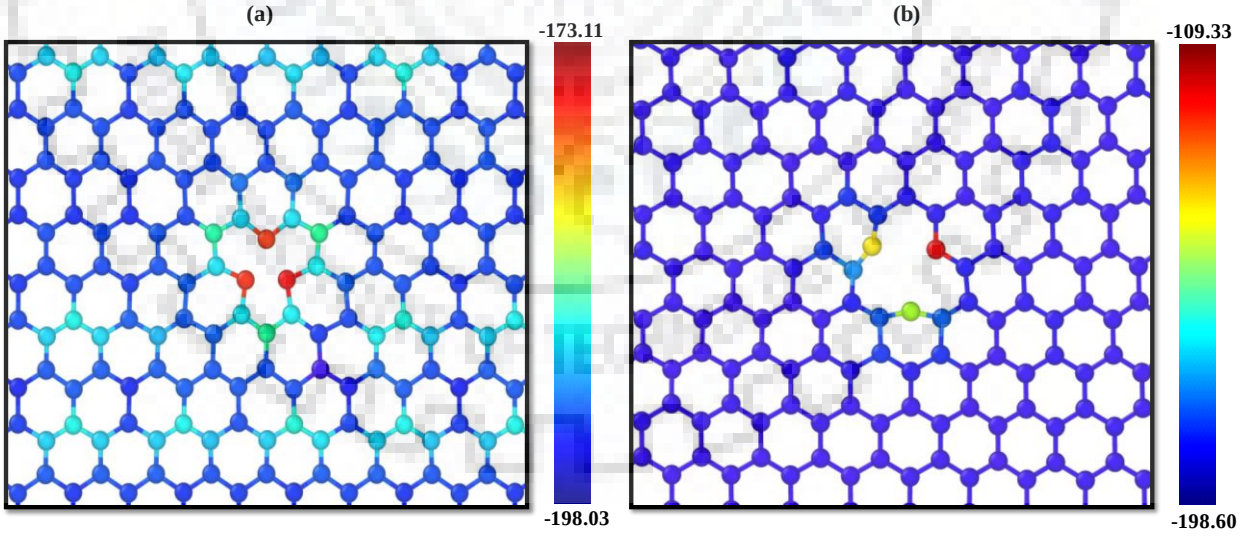

Fig.3.5 Potential energy distribution over the carbon atoms in the vicinity of vacancy created in (a) dry and (b) wet form of graphene

Displacement threshold energy

Simulations were performed to predict the displacement threshold energy for atoms in dry and wet form of graphene. Particular emphasis was laid to ensure negation of thermal effects such as formation of a sink at a constant temperature of 300K for calculation of displacement threshold energy. In order to negate the effect of temperature, multiple simulations were run in this stage with different PKA's and average was taken as E_d. It can be observed from Fig.6 that average E_d values for atoms in water submerged graphene (≈23.5eV) are higher as compared to dry graphene (≈19.8eV). The E_d values predicted in this dissertation in dry form of graphene are in good agreement with the previously reported values [35,37-38]. It can be inferred from the Fig.3.6 that graphene in water offers more resistance to any defect formation as compared to dry graphene.

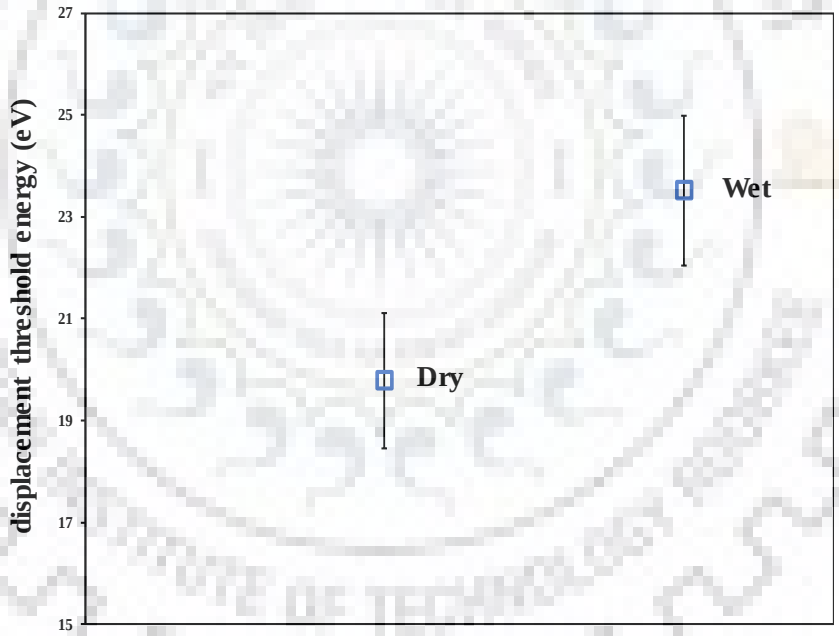

Fig. 3.6 Displacement threshold energy in dry and wet form of graphene

Grain boundary formation energy

In the last phase of the simulations, tilt symmetrical grain boundaries were generated in dry and wet form. The grain boundaries were created using the sewing method proposed by Xu et

al. [39]. Initially, simulations were performed with bi-crystalline graphene containing mis-orientation angles of 9.44°, 13.2° and 21.8°. The GB formation energy in dry state was predicted and was found in good agreement with the same calculated by Verma et al. [12] and Liu et al. [40]. Later on, GB formation energy was also estimated, while submerged in water and comparison was made in table3. It can be observed from the comparison in table 3 that GB formation energies are almost double in wet form, and the trend was independent to mis-orientation angle.

Table 3.1: GB formation energies for Dry and Submerged Graphene at various angles

S No.	Tilt angle	GBE(Dry graphene) in eV/nm	GBE (wet graphene) in eV/nm
(a)	9.44°	3.160	7.96577
(b)	13.2°	3.399	8.41446
(c)	21.8°	2.1844	5.384

Grain boundaries contains unfulfilled valencies, thus are potential sites for chemical reactions, corrosion, segregation of diffusing entities. Also, most dislocations get trapped at GB as higher activation energy is required to overcome them. There is a marked increase in grain boundary formation energies at various angles of orientation, while submerged in water as compared to dry state.

3.4 Summary

Molecular dynamics-based simulations were performed to study the defect formation dynamics in dry and wet form of graphene nanosheets. It can be concluded from the simulations that defective graphene nanosheets are more stable in water as compared to dry form. Potential energy distribution over the carbon atoms in the vicinity of vacancy was studied, and it was

predicted that presence of water molecules lowers the energy of edge atoms (surrounding vacancy defect) as compared to edge atoms in dry graphene nanosheets. Water molecules interacts with the atoms present at the edges of defects and helps in achieving minimum energy configuration. Similarly, non-bonded interaction forces exerted by water on graphene nanosheet increases the displacement threshold energy of graphene atoms. Resistance to defect formation was higher in water submerged graphene as compared to dry state.

3.5 References

[1] Mazdak Taghiokoui, Trends in Graphene Research, Materials Today,Volume 12, issue 10, Pages 34-37.October (2009)

[2] Novoselov K S, Geim A K, Morozov S V, Jiang D A, Zhang Y, Dubonos S V, Grigorieva I V and Firsov A. Electric field effect in atomically thin carbon films Science **306** 666–9(2004)

[3] Castro Neto, Antonio & Guinea, Francisco & Peres, Nuno & Novoselov, K.S. & Geim, A.K. The electronic properties of graphene. Review of Modern Physics. 81. 10.1103/RevModPhys.81.109. (2007)

[4] Molitor, F & Güttinger, Johannes & Stampfer, Christoph & Dröscher, S & Jacobsen, Arnhild & Ihn, Thomas & Ensslin, Klaus. Electronic properties of graphene nanostructures. Journal of physics. Condensed matter: An Institute of Physics journal. 23. 243201. 10.1088/0953-8984/23/24/243201. (2011)

[5] Graef H et al,Ultra-long wavelength Dirac plasmons in graphene capacitors J. Phys. Mater **1**01LT02,(2018)

[6] Geim AK and Novoselov KS, the rise of Graphene, Nat. Mater. **6** 183-91 (2007)

[7] Verma A and Parashar A, Reactive force field based atomistic simulations to study fracture toughness of bicrystalline graphene functionalised with oxide groups Diam. Relat. Mater. **88** 193–203(2018)

[8] Verma A and Parashar A, Molecular dynamics based simulations to study failure morphology of hydroxyl and epoxide functionalised graphene Comput. Mater. Sci. **143** 15–26(2018)

[9] Rajesh Kumar and Avinash P, Atomistic modeling of BN nanofillers for mechanical and thermal properties: a review, Nanoscale, 8, 22-49, (2016)

[10] Verma A, Parashar A and Packirisamy M , Atomistic modeling of graphene and hexagonal boron nitride polymer nanocomposites: a review Wiley Interdisciplinary Reviews: Computational Molecular Science **8** e1346(2018)

[11] Nakada K and Ishii A 2011 Migration of adatom adsorption on graphene using DFT calculation Solid State Commun. **151** 13–6

[12] Verma A, Parashar A and Packirisamy M 2018 Tailoring the failure morphology of 2D bicrystalline graphene oxide J. Appl. Phys. **124** 015102

[13] Achtyl J L et al 2015 Aqueous proton transfer across single-layer graphene Nat. Commun. **6** 6539

[14] Graphene Flagship. "Zero gravity: Graphene for space applications". ScienceDaily, 7 July 2017.

[15] Jaydevsinh M. Gohil, Akkihebbal K. Suresh, Chlorine attack on reverse osmosis membranes: Mechanisms and mitigation strategies, Journal of Membrane Science, 541, 108(2017)

[16] Boretti Albert, Al-Zubaidy Sarim, Vaclavikova Miroslava, Al-abri Mohammed,Castelletto Stefania, Mikhalovsky Sergey, Outlook for graphene-based desalination membranes, npj Clean Water,5.1.1,(2018)

[17] Janire Peña-Bahamonde, Hang N. Nguyen, Sofia K. Fanourakis and Debora F. Rodrigues, Recent advances in graphene-based biosensor technology with applications in life sciences, J Nanobiotechnol (2018)

[18] Zulfiqar H. Khan, Atieh R. Kermany, Andreas Öchsner, Francesca Iacopi, Mechanical and Electromechanical Properties of Graphene and their Potential Applications in MEMS, Journal of Physics D: Applied Physics, Volume 50, Issue 5, article id. 053003 (2017)

[19] AK Arun, G & Sreenivas, Nikhil & Brahma Reddy, Kesari & Sai Krishna Reddy, K & E Shashi Kumar, M & Pramod, R. (2018). Investigation on Mechanical Properties of Graphene Oxide reinforced GFRP. IOP Conference Series: Materials Science and Engineering. 310. 012158. 10.1088/1757-899X/310/1/012158.

[20] Park C, Yun G. Characterization of Interfacial Properties of Graphene-Reinforced Polymer Nanocomposites by Molecular Dynamics-Shear Deformation Model. ASME. J. Appl. Mech. 2018;85(9):091007-091007-10. doi:10.1115/1.4040480. (2018)

[21] Avouris P and Dimitrakopoulos C, Graphene: synthesis and applications Mater. Today **15** 86–97(2012)

[22] Yao, T., Xin, G., Scott, S. M., Gong, B., & Lian, J. (2018). Thermally-Conductive and Mechanically-Robust Graphene Nanoplatelet Reinforced UO2 Composite Nuclear Fuels. Scientific reports, 8(1), 2987. doi:10.1038/s41598-018-21034-4(2018)

[23] Genki Odahara, Tsuyoshi Ishikawa, Kazuya Fukase, Shigeki Otani, Chuhei Oshima, Masahiko Suzuki, Tsuneo Yasue and Takanori Koshikawa, Self-Standing Graphene Sheets Prepared with Chemical Vapor Deposition and Chemical Etching,Graphene – Synthesis,

Characterization, Properties and Applications, Edited by Jian Ru Gong p. cm. ISBN 978-953-307-292-0 (2011)

[24] Rajasekaran G, Narayanan P and Parashar A, Effect of point and line defects on mechanical and thermal properties of graphene: a review Crit. Rev. Solid State Mater. Sci. **41** 47–71(2016)

[25] Verma A and Parashar A, the effect of STW defects on the mechanical properties and fracture toughness of pristine and hydrogenated graphene Phys. Chem. Chem. Phys. **19** 16023–37(2017)

[26] Meng F, Chen C and Song J, Dislocation shielding of a nanocrack in graphene: atomistic simulations and continuum modeling The journal of physical chemistry letters **6** 4038–42(2015)

[27] Vibhor Singla, Akarsh Verma and Avinash Parashar, A molecular dynamics based study to estimate the point defects formation energies in graphene containing STW defects, Materials Research Express, Volume 6, Number 1, IOP science,(2018)

[28] Bellido E P and Seminario J M, Molecular dynamics simulations of ion-bombarded graphene The Journal of Physical Chemistry C **116** 4044–9, (2012)

[29] Yoon K et al Atomistic-scale simulations of defect formation in graphene under noble gas ion irradiation ACS Nano **10** 8376–84(2016)

[30] Merrill A, Cress C D, Rossi J E, Cox N D and Landi B J, Threshold displacement energies in graphene and single-walled carbon nanotubes Phys. Rev. B **92** 075404(2015)

[31] C.H.Wong, and V.Vijayaraghavan, "Transport characteristics of water molecules in carbon nanotubes investigated by using molecular dynamics simulation," Computational Materials Science Volume **89**, 36-44 (2014)

[32] David Cohen-Tanugi and Jeffrey C. Grossman, Mechanical Strength of Nanoporous Graphene as a Desalination Membrane, pubs.acs.org/NanoLett dx.doi.org/10.1021/nl502399y (2014)

[33] Senftle, Thomas P ,Hong, Sungwook ,Islam, Md Mahbubul,Kylasa, Sudhir B,Zheng, Yuanxia,Shin, Yun Kyung,Junkermeier, Chad,Engel-Herbert, Roman,Janik, Michael J, Aktulga, Hasan Metin,Verstraelen, Toon,Grama, Ananth,van Duin, Adri C T, The ReaxFF reactive force-field: development, applications and future directions, Npj Computational Materials,2,15011, (2016)

[34] Bharat Bhushan Sharma, and Avinash Parashar, "A review on thermo-mechanical properties of bi-crystalline and polycrystalline 2D nanomaterials," Critical reviews in solid state and materials science, doi.org/10.1080/10408436.2019.1582003 (2019)

[35] Krasheninnikov AV, Lehtinen PO, Foster A S and Nieminen RM, "Bending the rules: contrasting vacancy energetics and migration in graphite and carbon nanotubes," Chem. Phys. Lett. **418** 132–6 (2006)

[36] Thrower P A, and Mayer R M, "Point defects and self-diffusion in graphite," Physica Status Solidi (a) **47** 11–37 (1978)

[37] Zobelli A, Gloter A, Ewels CP, "Seifert G and ColliexC, Electron knock-on cross section of carbon and boron nitride nanotubes," Phys. Rev. B **75** 245402 (2007)

[38] Kotakoski J, Jin CH, Lehtinen O, Suenaga K and Krasheninnikov AV, Electron knock-on damage in hexagonal boron nitride monolayers Phys. Rev. B **82** 113404 (2010)

[39] N. Xu, J. G. Guo, and Z. Cui, "The influence of tilt grain boundaries on the mechanical properties of bicrystalline graphene nanoribbons," Physica E **84**, 168–174 (2016)

[40] H. K. Liu, Y. Lin, and S. N. Luo, "Grain boundary energy and grain size dependences of thermal conductivity of polycrystalline graphene," J. Phys. Chem. C **118** (42), 24797–24802 (2014)

Chapter 4

Mechanical and fracture behaviour of water submerged graphene[2]

4.1 Introduction

During the last couple of years, industries across the board are implementing graphene's futuristic traits and characteristics. Graphene is a two-dimensional material containing sp^2-hybridized carbon atoms. Due to exceptional mechanical, thermal and electrical properties, graphene is emerging as a potential candidate to develop cutting edge space technology [1], ultrafiltration membrane systems [2], nano-biotechnology [3], MEMS/NEMS (nano electromechanical systems) [4] and in other applications as well [5-9]. Lee et al. [10] experimentally measured the tensile strength of free-standing graphene, and reported as the strongest material. Liu et al.[11] investigated the effect of chirality on the tensile strength of graphene. Khare et al. [12] employed molecular dynamics (MD) based simulations to study the mechanical strength of graphene in conjunction with geometrical defects. Rajasekaran and Avinash [13] predicted shift in the failure morphology of graphene in presence of Stone-Thrower-Wales defects (STW). Akarsh and Avinash [14] have also predicted the effect of functionalized grain boundaries on the mechanical and fracture behavior of graphene. Tsai and Tu [15] investigated the mechanical properties of graphite flakes and single graphene layer with the help of MD based simulations. They predicted that graphene layers provide improved reinforcement effect in nanocomposites. The variation in the fracture strength of graphene with temperature, strain rate, and crack length were investigated by Zhao and Aluru [16] using the quantized fracture mechanics (QFM) theory. Zhang et al. [17] investigated the mechanical

[2] This chapter is an excerpt from the article accepted for publication as Saurabh S Sharma, Bharat Bhushan Sharma, Avinash Parashar, 2019, Journal of Applied Physics, JAP19-AR-00311R1

properties of bilayer graphene sheets using MD simulations. The above-mentioned literature demonstrates the exceptional mechanical qualities of graphene. Despite the fact that mechanical and fracture behaviour of graphene have already been investigated by many researchers, still the literature is limited on the properties of graphene submerged in water. Shortage of potable water in recent future is going to affect people all around the globe. Current production of potable water is primarily through reverse osmosis (RO) systems, and the demands of ever growing industry require better efficiency at lower cost. In order to improve the efficiency of desalination techniques, membranes with superior strength are required to be developed that can sustain higher pressure and increased output. Now, researchers are exploring the membrane capabilities of graphene for water desalination [18], ion separation [19] as well as for tissue engineering [20]. Jiao et al. [21] used MD based simulations to study the molecular permeation of gases through nano porous graphene. In another article, Wong and Vijayaraghavan [22] studied the mechanical strength of graphene submerged in water in conjunction with vacancy defects. In their atomistic simulations edge effects were ignored for submerged graphene. Tanugi and Grossman [23] have also investigated the mechanical strength of defective nanosheet of graphene submerged in water. Hu et al. [24] experimentally reported that graphene oxide membrane shows lower rejection rate for salt cations, but high-water flux through the membrane as compared to most of the other commercially available membranes. It was reported in the review article that graphene oxide has already been tested by many researchers for cation and ion rejection in water [25]. Water de-salination requires manufacturing of membranes with vacancies for filtration purpose [2,18,19]. Large-scale production of membrane sized graphene is a formidable challenge, and is achieved primarily through chemical vapour deposition (CVD) [26]. This introduces defects such as adatoms, vacancies and dislocations into graphene, which are precursors to the formation of voids and cracks in the material and results in a premature failure of these materials well below their

theoretical failure point. This mandates investigation of the fracture properties of graphene submerged in water. So far, literature is almost mute on the effect of water on the structural stability and fracture toughness of graphene. In this dissertation, authors have employed MD based atomistic simulations to study the mechanical and fracture behaviour of graphene submerged in water. In order to quantify the effect of water on the properties of graphene, results were compared with the pristine and dry form of graphene.

4.2 Modelling Details

A classical mechanics based approach was employed for studying the mechanical and fracture behaviour of graphene in dry and water submerged state. MD based simulations were carried out to capture the effect of water on the properties of graphene. An open source code LAMMPS (Large-scale Atomic/Molecular Massively Parallel Simulator) package was used to perform all the simulations. The authors have used hybrid type interatomic potential in the simulations performed with graphene submerged in water. In hybrid type potential, Adaptive intermolecular reactive empirical bond order (AIREBO) and TIP3P was used to simulate the bonded interaction in graphene (carbon carbon) and water (hydrogen and oxygen), whereas the non-bonded interactions between C, O, H atoms was simulated with the help of Lennard Jones potential (LJ 6-12). AIREBO force field was used to capture the interatomic interactions between carbon-carbon atoms in graphene. In order to avoid the spurious behavior of carbon–carbon bonds simulated with AIREBO, a single value for the cut-off function ~ 1.92 Å was used in all the simulations. Simulations were performed with graphene nanosheet having equal length and width ≈100 Å, which constitutes approximately 3922 carbon atoms. TIP3P potential was used in all the simulations to capture the bond dynamics between hydrogen and oxygen atoms in water. In order to avoid edge affects in graphene, periodic boundary conditions were imposed in all the principal directions. All the simulations were performed at the room

temperature of 300K. In order to perform the time integration in conjunction with Newtonian mechanics a uniform time step of 0.25fs was employed in equilibration and deformation stage.

Initially, energy of the atomic configuration was minimized at 0K with the help of conjugate gradient (CG) algorithm. After achieving minimum energy configuration, graphene nanosheet in conjunction with water or without water was equilibrated to room temperature of 300K, under the influence of NPT ensemble that exploits the Nośe–Hoover barostat and thermostat. After finishing relaxation of atoms for 12.5 ps, graphene sheet in pristine form or submerged in water was subjected to tensile deformation with a strain rate at 10^{-3} ps^{-1} under the influence of NVT ensemble. In order to investigate the deformation in dry and wet form of graphene, strain energy formulation in conjunction deformation was utilized. Strain energy formulation was performed with the help of potential energy of the required system as illustrated in Eq. 1 and Eq.2.

$$U_\epsilon = E_\epsilon - E_0 \quad (1)$$

where, E_o and E_ϵ are the potential energy of the atomic system after relaxation (ϵ =0) and at finite strain ϵ, respectively, whereas U_ϵ is the strain energy stored in graphene nanosheet. In order to calculate the fracture stress, polynomial of third order was fitted between strain energy and strain, and derivative of the same polynomial was used to get corresponding stresses, which is further illustrated in Eq. 2.

$$\sigma = \frac{1}{V_0}\frac{\partial U}{\partial \epsilon} \quad (2)$$

Where, σ is Cauchy stress component and V_0 is the volume of nanosheet. During all the simulations for studying tensile deformation or fracture toughness, graphene was only subjected to uniaxial deformation, hence stresses calculated with the help of eq. 2 corresponds to normal stress in the direction of deformation. As mode-I fracture toughness was predicted

in the dissertation, hence stresses normal to the crack edges was only considered. Authors have predicted Cauchy stress components in the simulations with the help of strain energy as described in Eq. 1 and Eq.2. In order to be consistent with the continuum principle of linear elastic fracture mechanics, authors have employed only Cauchy stress values for predicting stress intensity factor values (K_{IC}). Authors have estimated the Cauchy stress and atomistic stress response with respect to strain, and comparison is plotted in Fig.1. It can be inferred from the response plotted in Fig.1 that both the stresses are comparable, but the offset at higher strain values are due to higher simulation temperature of 300K, which induces the effect of kinetic energy in virial stress component. Similar kind of behaviour between the two stresses was observed in the work Nuwan Dewapriya [27]. It has also been reported in the work of Subramaniyan and Sun [28] that atomistic stresses directly calculated from the MD simulations are comparable to the Cauchy stresses at the continuum level.

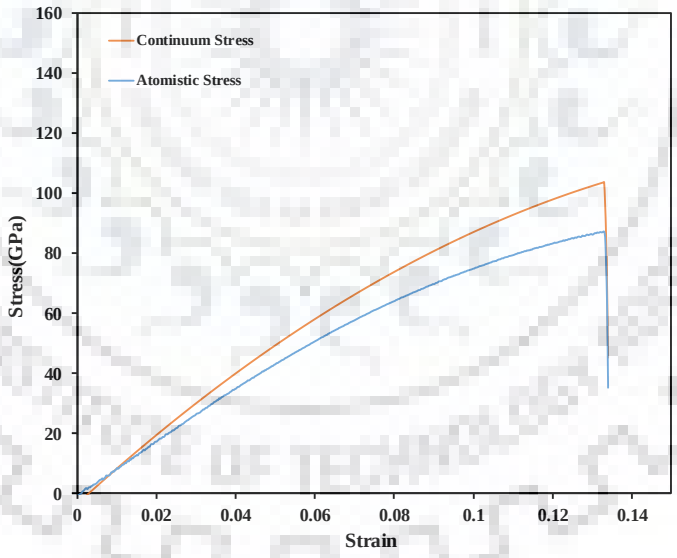

Fig. 4.1 Comparison between Cauchy and Atomistic Stresses

In addition to Cauchy stresses, authors have also estimated virial stresses with the help of Eq.3

$$\sigma_{ij}^{\alpha} = \frac{1}{\varphi^{\alpha}}\left(\frac{1}{2} m^{\alpha} v_i^{\alpha} v_j^{\alpha} + \sum_{\beta=1,n} r_{\alpha\beta}^{j} f_{\alpha\beta}^{i}\right) \quad (3)$$

Where v^{α} and m^{α} are the velocity and mass of atom α; $r_{\alpha\beta}$ is distance between the atoms α and β; φ^{α} is the volume of system; α and β being the atomic indices; i and j stand for indices in cartesian coordinate system.

Structural stability of dry and submerged graphene was predicted with the help of radial distribution function (RDF) estimated just after energy minimization. Vacancy formation energy (VFE) was estimated with the help of Eq.4 to understand the structural stability of graphene in terms of defect formation energies.

$$E_{vac} = E_f - E_i + E_{coh} \quad (4)$$

here, E_{vac} = vacancy formation energy, E_f = energy of the system after the formation of vacancy, E_i = energy of the system before the formation of vacancy, E_{coh} = cohesive energy of the system. In order to estimate the cohesive energy of carbon atom in dry and wet form of graphene, the atomic configuration in each case was energy minimized at 0K with the help of conjugate gradient algorithm. Potential energy of graphene was separately calculated in dry as well as wet state, and was divided by total number of carbon atoms in graphene to predict the cohesive energy of carbon in dry (E_{coh}=7.45eV) and wet state (E_{coh}=7.45eV). No significant difference in the values of cohesive energies was observed in dry and wet state of graphene. In order to validate the accuracy of simulations and interatomic potential used in the simulations, these values of cohesive energies were further compared with the first principle calculations/ DFT based simulations available in the literature [29,30], and were found in good agreement. Fracture toughness of dry and submerged graphene was predicted with the help of Eq.5.

$$K_{IC} = f\sigma\sqrt{\pi a} \quad (5)$$

Where, σ is the normal stress value at the instance of first bond rupture, a is half the central crack length, f ≈ 1, and K_{IC} is stress intensity factor. In order to fix the crack length, simulations were performed with different crack lengths, and concluded that beyond $2a$ = 21 Å, the K_{IC}

attains a constant value. Hence, for all the simulations the crack length was kept fixed at ≈ 20 Å.

4.3 Results and discussions

As mentioned in the previous section, simulations were performed in two stages; first stage of simulation helps in estimating the tensile deformation, whereas second stage corresponds to fracture toughness calculations for dry and submerged graphene. The simulation box containing dry and submerged graphene is shown in Fig. 4.2

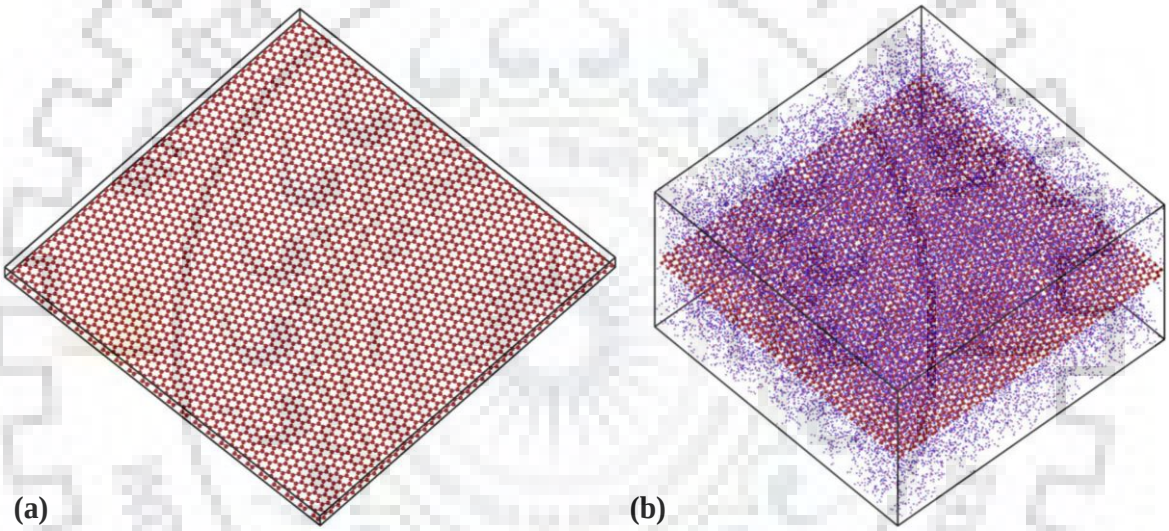

Fig. 4.2 Atomistic configurations of (a) dry and (b) submerged graphene nanosheets, respectively

4.3.1 Structural stability of graphene submerged in water

In order to study the structural stability, full width half maximum (FWHM) value of radial distribution function (RDF) was estimated for dry and wet graphene nanosheets with minimum energy configuration. after achieving minimum energy configuration. Higher value of FWHM corresponds to lower structural stability and vice versa. In addition to FWHM, molecular

statics-based simulations were also performed to predict the value of VFE in dry and water submerged graphene. The values of FWHM and VFE for dry and water submerged graphene are tabulated in table 4.1

Table 4.1. FWHM and VFE values of dry and water submerged graphene

GRAPHENE	FWHM	VFE(eV)
Dry	0.025	7.3
Submerged	0.049	7.2
Dry (Experimental)	-	7±0.5

It can be inferred from the FWHM values that the structural stability of graphene deteriorates in submerged water, whereas the structure of defective graphene is more stable in water as compared to dry state. A lower value of VFE indicates towards more stability for graphene in wet state as compared to dry state. After energy minimization of atomic configuration, bond lengths between carbon-carbon was estimated as 1.44 Å and 1.42 Å for wet and dry graphene, respectively. Increase in the bond length leads to pre-stressed condition in wet form of graphene. Generating vacancy in wet graphene helps in relieving these pre-stresses, which lowers the value of VFE in wet state as compared to dry state. As these simulations are molecular statics based, hence no effect of temperature was accounted in these calculations at 0K. In order to further emphasized our observations, forces experienced by graphene in dry and submerged condition at 0K and zero load are shown in Fig.4.3. It can be observed from Fig.4.3 that graphene sheet submerged in water experienced forces in all the principle directions, whereas under the same conditions dry sheet of graphene was experiencing zero forces.

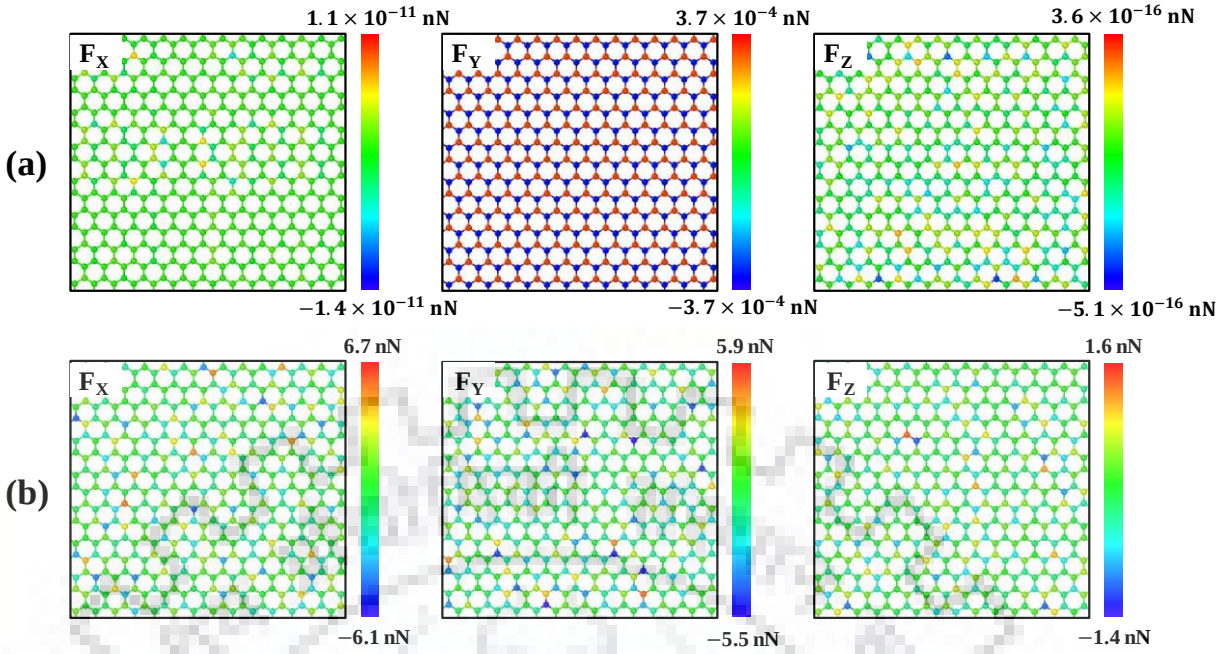

Fig. 4.3 Atomic force distribution after energy minimization corresponding to (a) dry and (b) submerged graphene nanosheets, respectively

After investigating the structural stability of graphene at zero load, next set of simulations were performed with atomic configuration subjected to tensile deformation in armchair (AC) and zig zag (ZZ) directions, respectively at a temperature of 300K. Distribution of strain energy with respect to strain is plotted in Fig.4 along AC and ZZ directions, respectively. It can be inferred from the strain energy trend that submerged graphene absorbed more energy before getting damaged as compared to dry graphene, and this trend was independent of chirality. Similar trends between strain energy and strain were observed in the work of Wong and Vijayaraghavan [22]. However, early failure in wet graphene nanosheet was predicted in Ref. [22], which can be attributed to the edge effects. In this work, authors have employed full graphene sheet with periodic boundary conditions, which helps in avoiding the edge effects.

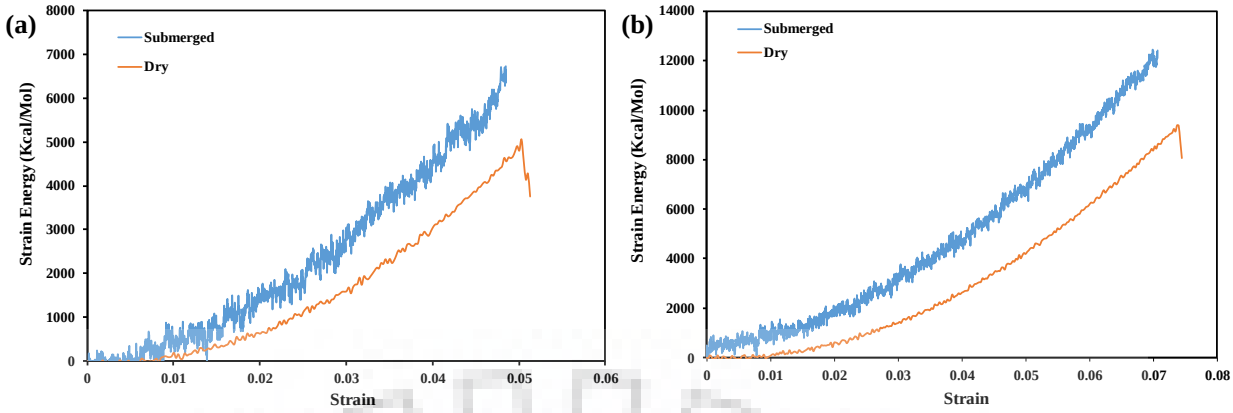

Fig. 4.4. Strain energy vs Strain response for dry and submerged graphene (a) AC and (b) ZZ directions, respectively

4.3.2 Fracture toughness of dry and water submerged graphene

Next set of simulations were performed to study the effect of water on the mode-I fracture behaviour of graphene in AC and ZZ directions. The schematic of crack in the graphene along AC and ZZ directions are shown in Fig.4.5. AC and ZZ in this subsection refers to the direction of loading. In order to satisfy the mode-I loading criterion, the uniaxial tensile load was always applied in the direction perpendicular to the crack edges.

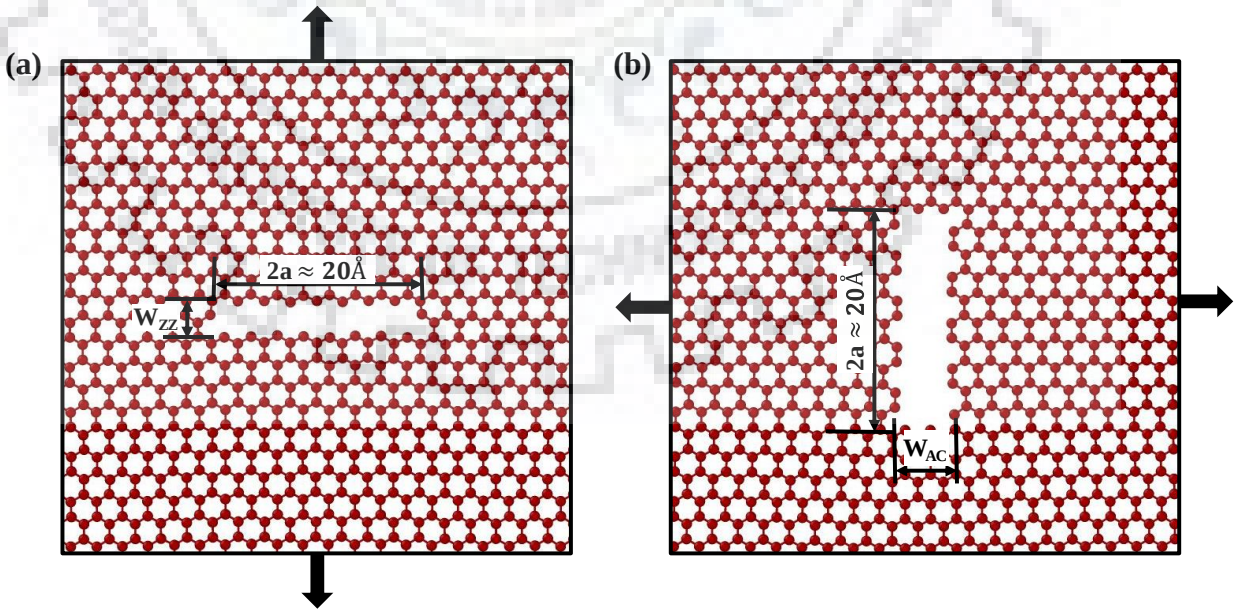

Fig. 4.5. Schematic of crack in graphene subjected to mode-I loading in (a) AC (b) ZZ directions, respectively

Fracture behaviour of dry and water submerged graphene was predicted at room temperature of 300K. The value of K_{IC} was estimated with the help of Eq.5. Fracture toughness of graphene in dry state was estimated as K_{IC} =1.84 K_{IC} (MPa√m) and K_{IC} = 2.905 (MPa√m) for AC and ZZ directions, respectively. Similar type of trend with higher stability for zig-zag edges were experimentally observed in the work of Girit, C. O. et al. [31]. Fracture toughness in terms of K_{IC} was estimated for dry and water submerged graphene, which is tabulated in table 4.2. It is pertinent to mention that the fracture toughness of water submerged graphene in AC direction improves, whereas an opposite trend was predicted for water submerged graphene in ZZ direction.

Table 4.2. Fracture toughness of dry and water submerged graphene in AC and ZZ directions

Type of graphene	**K_{IC} AC direction (MPa√m)**	**K_{IC} ZZ direction (MPa√m)**
Pristine dry	1.84	2.90
Pristine submerged	2.37	2.25
dry graphene (crack H passivated)	2.33	2.42
Submerged graphene (crack H passivated)	2.49	2.41

It can be inferred from K_{IC} values tabulated in table 2 that water has significantly affected the fracture toughness of graphene. Fracture toughness of water submerged graphene increased by almost 29% in AC direction, while it decreases by an extent of 22% in ZZ direction. Crack edge atoms react with the water molecules that generates out of plane displacement between the opposite crack edges. It was predicted from the atomistic simulations that higher values of out of plane displacement between crack edge atoms in ZZ direction reduces the fracture toughness of graphene, whereas lower values help in retaining or even increasing the fracture

toughness of graphene in AC direction. The out of plane displacement for different configurations of graphene is plotted in Fig.4.6. It can be inferred from Fig.6 that lower and higher values of out of plane displacement between crack edges corresponds to higher and lower fracture toughness, respectively.

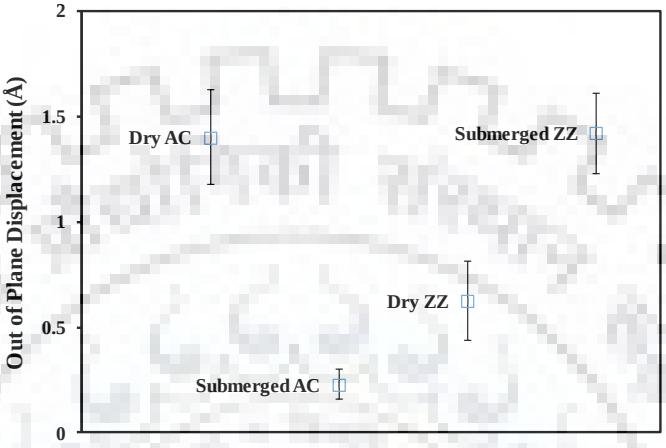

Fig. 4.6. Variation in out of plane displacement between the crack edges of graphene nanosheet in dry and wet state.

In order to capture the bond dynamics at the crack tip in dry and wet graphene, variation in the critical bond length was estimated and plotted in Fig.4.7. Here, critical refers to the bond from where crack starts propagating.

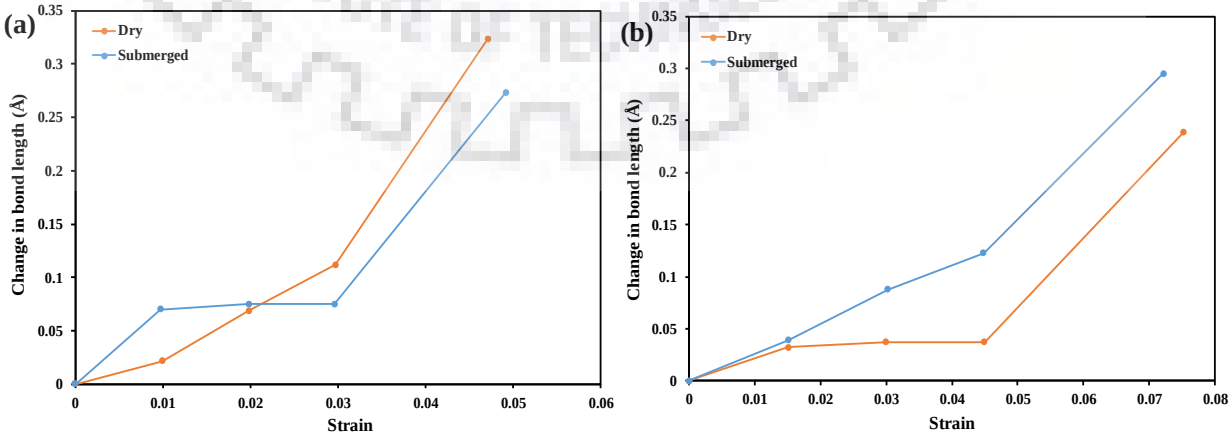

Fig. 4.7. Change in bond length for the critical bond at the crack tip as a function of applied strain corresponding to (a) AC direction and (b) ZZ direction, respectively.

It can be inferred from the trend plotted in Fig.4.7 that in water submerged graphene the variation in critical bond length was close to dry state in AC direction, whereas a significant gap in the variation between dry and submerged state was observed in ZZ direction. For water submerged graphene, crack propagation triggers at a lower critical bond length for ZZ direction as compared to AC direction. In addition to estimating the critical bond length at the crack tip, variation in the average atomic virial stress values at the crack tip in normalized condition is plotted in Fig.4.8. It can be observed in Fig.4.8a that lower crack tip stresses help in achieving higher fracture toughness for water submerged graphene in AC direction, whereas a contrasting trend was observed for the same in ZZ direction (Fig. 4.8b).

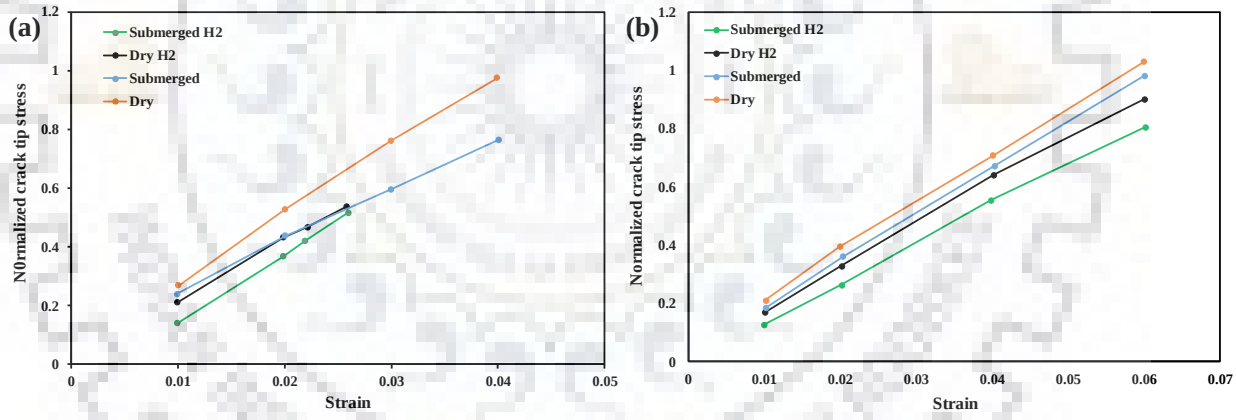

Fig. 4.8. Normalized crack tip stresses (a) AC (b) ZZ directions, respectively

Once more parameter that was attributed for the contrasting behaviour of fracture toughness in AC and ZZ direction of water submerged graphene was width of the crack. Due to crack healing observed in submerged graphene along ZZ direction, a higher width for the crack was considered, whereas no such phenomenon was observed in AC direction. Crack width in AC and ZZ direction was kept at 2.71 Å and 4.3 Å, respectively. In order to study the effect of crack width on the fracture toughness of dry and submerged graphene in AC direction, more

simulations were performed with varied crack width, and corresponding K_{IC} values were plotted in Fig.4.9. Interaction between crack edge atoms and water molecules have positive effect on the fracture toughness of graphene in AC direction, but that improvement starts reducing with the increase in crack width, which was eventually compensated by higher value of out of plane displacement between crack edge.

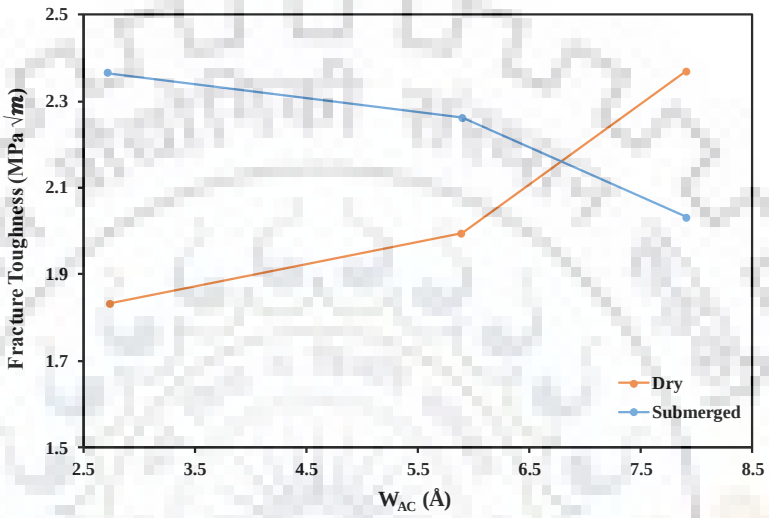

Fig. 4.9 Variation in fracture toughness with crack width along AC direction.

4.3.3 Effect of hydrogen passivation of crack edge atoms

In order to study the effect of interaction between the crack edge atoms and water molecules on the fracture toughness of graphene, edge atoms were hydrogen passivated to reduced their chemical reactivity. Effective functionalisation with hydrogen was achieved at a temperature of 300K. Hydrogen atoms were attached only to the carbon atoms at crack edge, changing their sp hybridization state to sp2 hybridisation state as illustrated in Fig.4.10

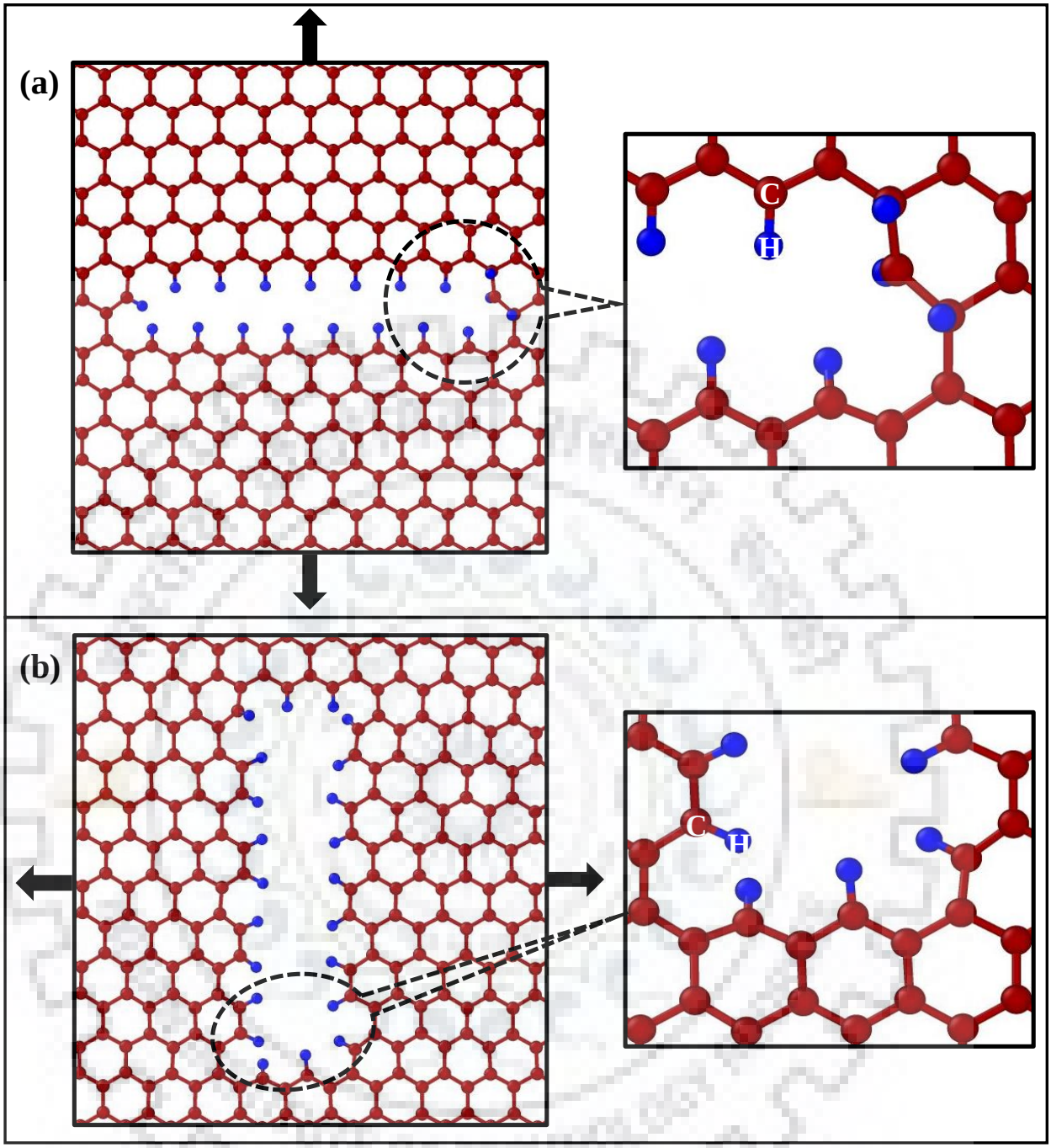

Fig. 4.10. Crack edge hydrogen passivation in (a) AC and (b) ZZ directions, respectively (red and blue atoms correspond to carbon and hydrogen, respectively)

Fracture toughness values of hydrogen passivated crack edge atoms in dry and wet graphene nanosheets are tabulated in table 4.2. It can be inferred from the K_{IC} values that hydrogen passivated crack edge atoms have lesser reactivity towards water molecules, hence the fracture toughness of graphene in dry and wet state was almost same. It can be observed from the crack

tip stresses plotted in Fig.4.8a that submerged graphene sheet with hydrogen passivation and dry pristine graphene in AC direction experienced minimum and maximum values respectively, which was supported by higher and lower values of fracture toughness, respectively. Similar kind of trend was observed in ZZ direction as well, higher crack tip stresses produce lower fracture toughness and vice versa.

4.4 Summary

Molecular dynamics-based simulations were performed to study the effect of water on the mechanical properties and fracture toughness of graphene nanosheet. It was predicted from the simulations that water has a significant impact on the structural stability and fracture toughness of graphene. Submergence of graphene in water is predicted to have a positive impact on the fracture toughness in AC direction, whereas deterioration effect in the zigzag direction was predicted, which could be attributed to higher out of plane displacement between the opposite crack edges in ZZ as compared to AC direction. The overall effect of water on the fracture toughness of graphene can be minimized with the help of hydrogen passivation of crack edge atoms.

4.5 References

[1] Graphene Flagship. "Zero gravity: Graphene for space applications". ScienceDaily, 7 July 2017. www.sciencedaily.com

[2] Jaydevsinh M. Gohil, Akkihebbal K. Suresh, Chlorine attack on reverse osmosis membranes: Mechanisms and mitigation strategies, Journal of Membrane Science, 541, 108 (2017)

[3] Janire Peña-Bahamonde, Hang N. Nguyen, Sofia K. Fanourakis and Debora F. Rodrigues, Recent advances in graphene-based biosensor technology with applications in life sciences, J Nanobiotechnol (2018)

[4] Zulfiqar H. Khan, Atieh R. Kermany, Andreas Öchsner, Francesca Iacopi, Mechanical and Electromechanical Properties of Graphene and their Potential Applications in MEMS, Journal of Physics D: Applied Physics, Volume 50, Issue 5, article id. 053003 (2017).

[5] Akarsh Verma, Avinash Parashar and M. Packirisamy, Atomistic modeling of graphene/ hexagonal boron nitride polymer nanocomposites: a review, WIREs Comput Mol Sci , e1346. doi: 10.1002/wcms.1346, (2017)

[6] Rajesh Kumar and Avinash Parashar, Atomistic modeling of BN nanofillers for mechanical and thermal properties: a review, Nanoscale, 8, 22-49, (2016)

[7] Akarsh Verma and Avinash Parashar, the effect of STW defects on the mechanical properties and fracture toughness of pristine and hydrogenated graphene. The Journal of Physical Chemistry C121 (1), 852-862 (2017).

[8] G. Rajasekaran, P. Narayanan and A. Parashar, Effect of point and line defects on mechanical and thermal properties of graphene: a review, Crit. Rev. Solid State Mater. Sci., 41(1), 47–71 (2016).

[9] G. Rajasekaran and A. Parashar, Molecular dynamics study on the mechanical response and failure behaviour of graphene: performance enhancement via 5–7–7–5 defects, RSC Adv., 26361–26373 (2016)

[10] Lee, C., Wei, X.D., Kysar, J.W. and Hone, J., Measurement of the Elastic Properties and Intrinsic Strength of Monolayer Graphene. Science, 321, 385-388 (2008)

[11] F. Liu, P.M. Ming, J. Li, Ab initio calculation of ideal strength and phonon instability of graphene under tension, Phys. Rev. B, 76 p. 064120 (2007),

[12] R. Khare, S.L. Mielke, J.T. Paci, S.L. Zhang, R. Ballarini, G.C. Schatz, T. Belytschko,

Physical Review B 75 (7), 075412, 2007. 280 (2007)

[13] G Rajasekaran and Avinash Parashar, Anisotropic compressive response of Stone–Thrower–Wales defects in graphene: A molecular dynamics study, Mater. Res. Express, 3 (9), 095015 (2016)

[14] Akarsh Verma, Avinash Parashar Reactive force field based atomistic simulations to study fracture toughness of bicrystalline graphene functionalised with oxide groups. Diamond and Related Materials, 88, 193-203. (2018)

[15] J.L. Tsai, J.F. Tu, characterizing mechanical properties of graphite using molecular dynamics simulation, Mater. Des., 31, pp. 194-199 (2010)

[16] H. Zhao, N.R. Aluru J., Temperature and strain-rate dependent fracture strength of graphene, Appl. Phys., 108, p. 064321 (2010)

[17] Y.Y. Zhang, C.M. Wang, Y. Cheng, Y. Xiang , Mechanical properties of bilayer graphene sheets coupled by sp^3 bonding, Carbon, 49, pp. 4511-4517 (2011)

[18] You, Yi &, V.Sahajwalla & Yoshimura, Masamichi & Joshi, Rakesh, Graphene and Graphene Oxide for Desalination. Nanoscale. 10.1039/C5NR06154G (2016).

[19] Song, Xinyi & Lu, Linghong & Wei, Mingjie & Dai, Zhongyang & Wang, Shanshan. Molecular dynamics simulations on the water flux in different two-dimension materials. Molecular Simulation, 6(8), (2018).

[20] SuRyonShin, Yi-ChenLi, Hae LinJang, Parastoo Khoshakhlagh, Mohsen Akbari, Amir Nasajpour, Yu Shrike Zhang, Ali Tamayol, Ali Khadem hosseini, Graphene-based materials for tissue engineering, Advanced Drug Delivery Reviews Volume 105, Part B, Pages 255-274 (2016).

[21] Jiao, Shuping & Xu Zhiping. Selective Gas Diffusion in Graphene Oxides Membranes: A Molecular Dynamics Simulations Study. ACS applied materials & interfaces. 7, 17, 9052-9059 (2015).

[22] C.H.Wong, V. Vijayaraghavan, Transport characteristics of water molecules in carbon nanotubes investigated by using molecular dynamics simulation, Computational Materials Science Volume 89, 15 June 2014, Pages 36-44 (2014).

[23] David Cohen-Tanugi and Jeffrey C. Grossman, Mechanical Strength of Nanoporous Graphene as a Desalination Membrane, Nano Lett. 2014, 14, 11, 6171-6178 (2014).

[24] Hu, M., Mi, B.X, Enabling graphene oxide nanosheets as water separation membranes. Environ. Sci. Technol., 47, 3715–3723 (2013).

[25] Zhuqing Wang, Aiguo Wu, Lucio Colombi Ciacchi, and Gang Wei, Recent Advances in Nanoporous Membranes for Water Purification. Nanomaterials.8,65 (2018).

[26] Dipankar Kalita. Graphene produced by chemical vapor deposition: from control and understanding of atomic scale defects to production of macroscale functional devices. Condensed Matter [cond-mat]. Université Grenoble Alpes, (2015).

[27] Dewapriya M, Molecular dynamics study of effects of geometric defects on the mechanical properties of graphene (MASc Thesis) *The University of British Columbia*, Canada (2012).

[28] Arun K. Subramaniyan, C.T. Sun, Continuum interpretation of virial stress in molecular simulations. International Journal of Solids and Structures 45 4340–4346 (2008).

[29] Shin H, Kang S, Koo J, Lee H, Kim J and Kwon Y. Cohesion energetics of carbon allotropes: Quantum Monte Carlo study J. Chem.Phys. 140 114702 (2014)

[30] Ivanovskaya V., Zobelli A., Teillet-Billy D., N. Rougeau, V. Sidis, P. R. Briddon Hydrogen adsorption on graphene: a first principles study, Eur. Phys. J. B 76: 481 (2010)

[31] Çağlar Ö. Girit, Jannik C. Meyer, Rolf Erni, Marta D. Rossell, C. Kisielowski, Li Yang, Cheol-Hwan Park, M. F. Crommie, Marvin L. Cohen, Steven G. Louie, A. Zettl, Graphene at the Edge: Stability and Dynamics, *Science* Vol. 323, Issue 5922, pp. 1705-1708 (2009)

Chapter 5

Conclusions and Future Aspects

5.1 Conclusions

This dissertation work discusses an exhaustive study performed to study the effects of fluidic media namely water on mechanical and fracture properties of graphene. Molecular dynamics-based simulations have been performed in conjunction with AIREBO and ReaxFF and TiP3P potentials to simulate graphene submerged in water model. Simulations were performed to study the effect of defects such as cracks and vacancies on the mechanical properties, fracture toughness and failure morphology of graphene sheet. The key findings and detailed conclusions from this thesis are summarized as follows.

- Literature review on defective graphene nanosheets helps in identifying the gaps in already performed work. It can be concluded from the literature review that classical mechanics based approach is more suitable to characterize pristine as well as defective sheets of graphene. In addition to that a single cutoff function is more suitable to predict the practical and realistic properties of graphene.
- As success of any MD simulation entirely depends on the type of interatomic potential employed for estimating interatomic forces, hence, AIREBO potential, which is capable of capturing the bond breaking in graphene is opted as a suitable potential for all the simulations performed in this research work. To validate the results ReaxFF and TiP3P potentials were used in conjunction.
- Synthesizing pristine graphene nanofillers is a rather hypothetical concept. Production techniques such as CVD inadvertently introduce different types of geometrical defects in the synthesized nanofillers. Defects such as vacancies and cracks deteriorate the mechanical properties of graphene. Stress fields in the vicinity of crack tips were used to predict the failure morphology of graphene nanosheet.
- It was predicted from the simulations that water has a significant impact on the structural stability and fracture toughness of graphene. Submergence of graphene in water is predicted to have a positive impact on the fracture toughness in AC direction, whereas deterioration effect in the zigzag direction was predicted, which could be attributed to higher out of plane displacement between the opposite crack edges in ZZ

as compared to AC direction. The overall effect of water on the fracture toughness of graphene can be minimized with the help of hydrogen passivation of crack edge atoms.

- It can be concluded from the simulations that defective graphene nanosheets are more stable in water as compared to dry form. Potential energy distribution over the carbon atoms in the vicinity of vacancy was studied, and it was predicted that presence of water molecules lowers the energy of edge atoms (surrounding vacancy defect) as compared to edge atoms in dry graphene nanosheets. Water molecules interacts with the atoms present at the edges of defects and helps in achieving minimum energy configuration. Similarly, non-bonded interaction forces exerted by water on graphene nanosheet increases the displacement threshold energy of graphene atoms. Resistance to defect formation was higher in water submerged graphene as compared to dry state.

Finally, it can be concluded from this research work that interaction with a fluidic media (water) has a potential to tailor mechanical properties, failure morphology and fracture toughness of graphene sheet.

5.2 Future Aspects

In this research project, effect of submergence in water on graphene nanosheet has been studied. Effect of a corrosive and or abrasive media such a sea water remains to be explored. Also, I have studied the formation of vacancy in submerged graphene nanosheet, while bombardment of an external ion on the nanosheet is yet to be carried out. Study of reinforcement of polymers with graphene nanofillers is the nascent stage. And future prospects include an upheaval in the field of de salination due to advent of graphene in the filtration systems. There is a lot yet to be achieved in the research on graphene and I believe we have just begun to scratch the surface of this new ocean of opportunities.